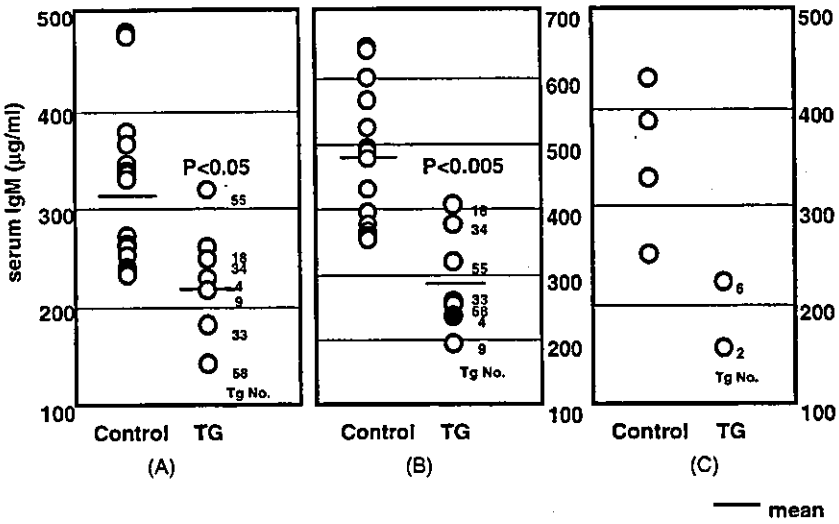

Fig. 5. Serum IgM levels in GFPmutRAG1 mice at 5 (A) and 8 weeks (B). (C) Sera from TG and their littermates from lineage no. 4 F1 mice were tested by ELISA for IgM (shown in μg/ml).

4. Discussion

4.1. RAG1 mutants inhibit recombination by wild RAG1 in vitro

To inhibit the V(D)J recombination, we generated catalytic RAG1 mutants with normal DNA binding activities as competitors for the endogenous RAG1 protein. Landree et al. (1999) and Kim et al. (1999) used site-directed mutagenesis to identify three RAG1 mutants in mice that bound DNA normally, but lacked DNA cleavage activity. We constructed seven RAG1 mutants making use of these previously identified mutations (D602A, D710A, and E964A). As expected, our mutants exhibited no recombination activity and inhibited recombination of an artificial substrate by wild type RAG1 in co-transfection experiments. These results suggest that RAG1 mutants bind to RSS together with the RAG2 protein and other protein partners but prevent the cleavage step of recombination. Unfortunately, the presence of equivalent amount of mutants and the wild type only inhibited recombination by 50%, indicating that mutants were not acting in a dominant negative fashion against wild type RAG1.

Sadofsky et al. (1993) reported that RAG1 protein was transported to the nucleus and rapidly degraded, with a half-life of 15 min. We also observed weak expression of full-length RAG1 protein in transiently transfected cells (Fig. 4A). Thus, we tried to prolong the half-life of mutants to provide them a functional advantage over wild type RAG1. RAG1 core protein (mouse residues 384–1008) truncated at both the N- and C-termini, has been reported to be highly stable (McMahan et al., 1997; Steen et al., 1999), and deletion of amino acid residues 15–79 (in human) increased protein levels (Silver et al., 1993). In agreement with previous studies, the steady state level of GFPwtRAG1, with its N-terminal domain (residues 1–379) replaced by GFP protein, was apparently higher than that of the wild type (Fig. 4A), which might account for its twofold greater ability to recombine the artificial substrate (Fig. 4B). Likewise, the GFPmutRAG1 triple point mutant showed a twofold increase in its recombination inhibition activity (Fig. 4C). RAG1 protein contains a Ring finger domain at residues 292–330 and many Ring finger proteins act as E3 ubiquitin protein ligases that bind to both target proteins and ubiquitin E2 conjugating enzymes (Joazeiro et al., 1999; Lorick et al., 1999; Waterman et al., 1999; Yokouchi et al., 1999). While ligase activity of RAG1 protein has not been reported, the Ring finger domain of RAG1 protein might promote the ubiquitination of RAG1 and/or other components of recombination complexes.

Previous studies have shown that the truncation of the N-terminus of RAG1 reduced its recombination activity (McMahan et al., 1997; Roman et al., 1997; Steen et al., 1999). Although the catalytic activity of GFPwtRAG1 was not determined in this study, the large increase in GFPwtRAG1 protein stability was not associated with a similar increase in its effect on recombination, suggesting that its catalytic activity might be reduced compared to the wild type protein. A zinc-finger motif (residues 292–330) is believed to participate in RAG1 dimerization (Bellon et al., 1997; Rodgers et al., 1996) and N-terminal truncation of RAG1 could conceivably affect the disassembly of the intermediate complexes and cording joint formation (Steen et al., 1999). The truncation of the N-terminus of RAG1 might alter its affinity for the recombination complex and/or DNA.

4.2. Transgenic mice carrying GFPmutRAG1 gene showed low serum IgM levels

Among seven transgenic mice carrying the GFPmutRAG1 gene, four (no. 4, 9, 33, and 58) showed a particularly

significant reduction of serum IgM levels, to approximately 33–50% of control levels. In lineage no. 4, progeny that inherited the GFPmutRAG1 gene also showed low serum IgM levels. These data suggested that the mutant RAG1 protein competed with the endogenous RAG1 protein for binding to recombination signal sequences at the immunoglobulin gene loci, resulting in the partial blockage of V(D)J recombination. However, the immunodeficient phenotypes were less dramatic than expected from the data on the mutant obtained in the in vitro assays. The serum IgG levels of the transgenic mice were indistinguishable from their littermates. The size of spleen and thymus of transgenic mice was equal to that of wild mice, and flow cytometric analysis of these tissues using antibodies recognizing lineage markers demonstrated normal lymphocyte profiles (data not shown). Although amino acid sequence of rabbit RAG1 shows high homology (89.2%) with a mouse RAG1, heterologous proteins might be due to the inefficiency of the inhibition. We are currently attempting to generate mouse expressing high levels of the mutant RAG1 protein and rabbit transgenic lines. In combination with the RAG1 mutant, other mutant proteins involved in V(D)J recombination, such as RAG2 and DNA-PK, might allow us to produce more severe immunodeficiency.

Evidence for the existence of somatic stem cells for most tissues has recently been described (Jiang et al., 2002; Krause et al., 2001). As with ES cells, such cells were expected to have therapeutic utility for tissue repair and organ regeneration. However, it is quite difficult to generate functional solid organs from stem cells in vitro. Our strategy to generate human-livestock animal hybrid organs by IUM will be applicable for stem cell therapy in the future.

Acknowledgements

This work was supported by Organized Research Combination System (ORCS) sponsored by Science and Technology Agency of Japan.

References

Aidinis, V., Dias, D.C., Gomez, C.A., Bhattacharyya, D., Spanopoulou, E., Santagata, S., 2000. Definition of minimal domains of interaction within the recombination-activating genes 1 and 2 recombinase complex. J. Immunol. 164, 5826–5832.

Bellon, S.F., Rodgers, K.K., Schatz, D.G., Coleman, J.E., Steitz, T.A., 1997. Crystal structure of the RAG1 dimerization domain reveals multiple zinc-binding motifs including a novel zinc binuclear cluster. Nat. Struct. Biol. 4, 586–591.

Dai, Y., Vaught, T.D., Boone, J., Chen, S.H., Phelps, C.J., Ball, S., Monahan, J.A., Jobst, P.M., McCreath, K.J., Lamborn, A.E., Cowell-Lucero, J.L., Wells, K.D., Colman, A., Polejaeva, I.A., Ayares, D.L., 2002. Targeted disruption of the α1,3-galactosyltransferase gene in cloned pigs. Nat. Biotechnol. 20, 251–255.

Enosawa, S., Miyashita, T., Fujita, Y., Suzuki, S., Amemiya, H., Omasa, T., Hiramatsu, S., Suga, K., Matsumura, T., 2001a. In vivo estimation of bioartificial liver with recombinant HepG2 cells using pigs with ischemic liver failure. Cell Transplant 10, 429–433.

Enosawa, S., Miyashita, T., Tanaka, H., Li, X., Suzuki, S., Amemiya, H., Omasa, T., Suga, K., Matsumura, T., 2001b. Prolongation of survival of pigs with ischemic liver failure by treatment with a bioartificial liver using glutamine synthetase transfected recombinant HepG2. Transplant Proc. 33, 1945–1947.

Fujino, M., Li, X.K., Suda, T., Hashimoto, M., Okabe, K., Yaginuma, H., Mikoshiba, K., Guo, L., Okuyama, T., Enosawa, S., Amemiya, H., Amano, T., Suzuki, S., 2001. In vitro prevention of cell-mediated xeno-graft rejection via the Fas/FasL-pathway in CrmA-transducted porcine kidney cells. Xenotransplantation 8, 115–124.

Gao, Y., Chaudhuri, J., Zhu, C., Davidson, L., Weaver, D.T., Alt, F.W., 1998a. A targeted DNA-PKcs-null mutation reveals DNA-PK-independent functions for KU in V(D)J recombination. Immunity 9, 367–376.

Gao, Y., Sun, Y., Frank, K.M., Dikkes, P., Fujiwara, Y., Seidl, K.J., Sekiguchi, J.M., Rathbun, G.A., Swat, W., Wang, J., Bronson, R.T., Malynn, B.A., Bryans, M., Zhu, C., Chaudhuri, J., Davidson, L., Ferrini, R., Stamato, T., Orkin, S.H., Greenberg, M.E., Alt, F.W., 1998b. A critical role for DNA end-joining proteins in both lymphogenesis and neurogenesis. Cell 95, 891–902.

Gu, Y., Seidl, K.J., Rathbun, G.A., Zhu, C., Manis, J.P., van der Stoep, N., Davidson, L., Cheng, H.L., Sekiguchi, J.M., Frank, K., Stanhope-Baker, P., Schlissel, M.S., Roth, D.B., Alt, F.W., 1997. Growth retardation and leaky SCID phenotype of Ku70-deficient mice. Immunity 7, 653–665.

Jiang, Y., Jahagirdar, B.N., Reinhardt, R.L., Schwartz, R.E., Keene, C.D., Ortiz-Gonzalez, X.R., Reyes, M., Lenvik, T., Lund, T., Blackstad, M., Du, J., Aldrich, S., Lisberg, A., Low, W.C., Largaespada, D.A., Verfaillie, C.M., 2002. Pluripotency of mesenchymal stem cells derived from adult marrow. Nature 418, 41–49.

Joazeiro, C.A., Wing, S.S., Huang, H., Leverson, J.D., Hunter, T., Liu, Y.C., 1999. The tyrosine kinase negative regulator c-Cbl as a RING-type, E2-dependent ubiquitin-protein ligase. Science 286, 309–312.

Kim, D.R., Dai, Y., Mundy, C.L., Yang, W., Oettinger, M.A., 1999. Mutations of acidic residues in RAG1 define the active site of the V(D)J recombinase. Genes Dev. 13, 3070–3080.

Krause, D.S., Theise, N.D., Collector, M.I., Henegariu, O., Hwang, S., Gardner, R., Neutzel, S., Sharkis, S.J., 2001. Multi-organ, multi-lineage engraftment by a single bone marrow-derived stem cell. Cell 105, 369–377.

Lai, L., Kolber-Simonds, D., Park, K.W., Cheong, H.T., Greenstein, J.L., Im, G.S., Samuel, M., Bonk, A., Rieke, A., Day, B.N., Murphy, C.N., Carter, D.B., Hawley, R.J., Prather, R.S., 2002. Production of α-1,3-galactosyltransferase knockout pigs by nuclear transfer cloning. Science 295, 1089–1092.

Landree, M.A., Wibbenmeyer, J.A., Roth, D.B., 1999. Mutational analysis of RAG1 and RAG2 identifies three catalytic amino acids in RAG1 critical for both cleavage steps of V(D)J recombination. Genes Dev. 13, 3059–3069.

Lei, G., Amemiya, H., Suzuki, S., Goto, T., Kokubo, T., Miyamoto, M., Kimura, H., 2000. New immunosuppressive reagent, FTY 720, spares immunologic memory. Transpl. Proc. 32, 1628.

Li, W., Chang, F.C., Desiderio, S., 2001. Rag-1 mutations associated with B-cell-negative scid dissociate the nicking and transesterification steps of V(D)J recombination. Mol. Cell Biol. 21, 3935–3946.

Lin, J.M., Landree, M.A., Roth, D.B., 1999. V(D)J recombination catalyzed by mutant RAG proteins lacking consensus DNA-PK phosphorylation sites. Mol. Immunol. 36, 1263–1269.

Lorick, K.L., Jensen, J.P., Fang, S., Ong, A.M., Hatakeyama, S., Weissman, A.M., 1999. RING fingers mediate ubiquitin-conjugating enzyme (E2)-dependent ubiquitination. Proc. Natl. Acad. Sci. U.S.A. 96, 11364–11369.

Max, E.E., Seidman, J.G., Leder, P., 1979. Sequences of five potential recombination sites encoded close to an immunoglobulin kappa constant region gene. Proc. Natl. Acad. Sci. U.S.A. 76, 3450–3454.

McBlane, J.F., van Gent, D.C., Ramsden, D.A., Romeo, C., Cuomo, C.A., Gellert, M., Oettinger, M.A., 1995. Cleavage at a V(D)J recombination signal requires only RAG1 and RAG2 proteins and occurs in two steps. Cell 83, 387–395.

McMahan, C.J., Difilippantonio, M.J., Rao, N., Spanopoulou, E., Schatz, D.G., 1997. A basic motif in the N-terminal region of RAG1 enhances V(D)J recombination activity. Mol. Cell Biol. 17, 4544–4552.

Miyazaki, J., Takaki, S., Araki, K., Tashiro, F., Tominaga, A., Takatsu, K., Yamamura, K., 1989. Expression vector system based on the chicken β-actin promoter directs efficient production of interleukin-5. Gene 79, 269–277.

Mombaerts, P., Iacomini, J., Johnson, R.S., Herrup, K., Tonegawa, S., Papaioannou, V.E., 1992. RAG-1-deficient mice have no mature B and T lymphocytes. Cell 68, 869–877.

Noordzij, J.G., Verkaik, N.S., Hartwig, N.G., de Groot, R., van Gent, D.C., van Dongen, J.J., 2000. N-terminal truncated human RAG1 proteins can direct T-cell receptor but not immunoglobulin gene rearrangements. Blood 96, 203–209.

Oettinger, M.A., 1992. Activation of V(D)J recombination by RAG1 and RAG2. Trends Genet. 8, 413–416.

Onishi, A., Iwamoto, M., Akita, T., Mikawa, S., Takeda, K., Awata, T., Hanada, H., Perry, A.C., 2000. Pig cloning by microinjection of fetal fibroblast nuclei. Science 289, 1188–1190.

Polejaeva, I.A., Chen, S.H., Vaught, T.D., Page, R.L., Mullins, J., Ball, S., Dai, Y., Boone, J., Walker, S., Ayares, D.L., Colman, A., Campbell, K.H., 2000. Cloned pigs produced by nuclear transfer from adult somatic cells. Nature 407, 86–90.

Rodgers, K.K., Bu, Z., Fleming, K.G., Schatz, D.G., Engelman, D.M., Coleman, J.E., 1996. A zinc-binding domain involved in the dimerization of RAG1. J. Mol. Biol. 260, 70–84.

Roman, C.A., Cherry, S.R., Baltimore, D., 1997. Complementation of V(D)J recombination deficiency in RAG-1(–/–) B cells reveals a requirement for novel elements in the N-terminus of RAG-1. Immunity 7, 13–24.

Rosengard, A.M., Cary, N.R., Langford, G.A., Tucker, A.W., Wallwork, J., White, D.J., 1995. Tissue expression of human complement inhibitor, decay-accelerating factor, in transgenic pigs. A potential approach for preventing xenograft rejection. Transplantation 59, 1325–1333.

Sadofsky, M.J., Hesse, J.E., McBlane, J.F., Gellert, M., 1993. Expression and V(D)J recombination activity of mutated RAG-1 proteins. Nucleic Acids Res. 21, 5644–5650.

Sakano, H., Huppi, K., Heinrich, G., Tonegawa, S., 1979. Sequences at the somatic recombination sites of immunoglobulin light-chain genes. Nature 280, 288–294.

Schatz, D.G., Oettinger, M.A., Baltimore, D., 1989. The V(D)J recombination activating gene, RAG-1. Cell 59, 1035–1048.

Schwarz, K., Gauss, G.H., Ludwig, L., Pannicke, U., Li, Z., Lindner, D., Friedrich, W., Seger, R.A., Hansen-Hagge, T.E., Desiderio, S., Lieber, M.R., Bartram, C.R., 1996. RAG mutations in human B cell-negative SCID. Science 274, 97–99.

Shinkai, Y., Rathbun, G., Lam, K.P., Oltz, E.M., Stewart, V., Mendelsohn, M., Charron, J., Datta, M., Young, F., Stall, A.M., et al., 1992. RAG-2-deficient mice lack mature lymphocytes owing to inability to initiate V(D)J rearrangement. Cell 68, 855–867.

Silver, D.P., Spanopoulou, E., Mulligan, R.C., Baltimore, D., 1993. Dispensable sequence motifs in the *RAG*-1 and *RAG*-2 genes for plasmid V(D)J recombination. Proc. Natl. Acad. Sci. U.S.A. 90, 6100–6104.

Steen, S.B., Han, J.O., Mundy, C., Oettinger, M.A., Roth, D.B., 1999. Roles of the "dispensable" portions of RAG-1 and RAG-2 in V(D)J recombination. Mol. Cell Biol. 19, 3010–3017.

Tonegawa, S., 1983. Somatic generation of antibody diversity. Nature 302, 575–581.

Villa, A., Santagata, S., Bozzi, F., Giliani, S., Frattini, A., Imberti, L., Gatta, L.B., Ochs, H.D., Schwarz, K., Notarangelo, L.D., Vezzoni, P., Spanopoulou, E., 1998. Partial V(D)J recombination activity leads to Omenn syndrome. Cell 93, 885–896.

Villa, A., Sobacchi, C., Notarangelo, L.D., Bozzi, F., Abinun, M., Abrahamsen, T.G., Arkwright, P.D., Baniyash, M., Brooks, E.G., Conley, M.E., Cortes, P., Duse, M., Fasth, A., Filipovich, A.M., Infante, A.J., Jones, A., Mazzolari, E., Muller, S.M., Pasic, S., Rechavi, G., Sacco, M.G., Santagata, S., Schroeder, M.L., Seger, R., Strina, D., Ugazio, A., Valiaho, J., Vihinen, M., Vogler, L.B., Ochs, H., Vezzoni, P., Friedrich, W., Schwarz, K., 2001. VDJ recombination defects in lymphocytes due to RAG mutations: severe immunodeficiency with a spectrum of clinical presentations. Blood 97, 81–88.

Waterman, H., Levkowitz, G., Alroy, I., Yarden, Y., 1999. The RING finger of c-Cbl mediates desensitization of the epidermal growth factor receptor. J. Biol. Chem. 274, 22151–22154.

Yarnell Schultz, H., Landree, M.A., Qiu, J.X., Kale, S.B., Roth, D.B., 2001. Joining-deficient RAG1 mutants block V(D)J recombination in vivo and hairpin opening in vitro. Mol. Cell 7, 65–75.

Yokouchi, M., Kondo, T., Houghton, A., Bartkiewicz, M., Horne, W.C., Zhang, H., Yoshimura, A., Baron, R., 1999. Ligand-induced ubiquitination of the epidermal growth factor receptor involves the interaction of the c-Cbl RING finger and UbcH7. J. Biol. Chem. 274, 31707–31712.

Zhu, C., Bogue, M.A., Lim, D.S., Hasty, P., Roth, D.B., 1996. Ku86-deficient mice exhibit severe combined immunodeficiency and defective processing of V(D)J recombination intermediates. Cell 86, 379–389.

CLONING AND STEM CELLS
Volume 5, Number 2, 2003

In Vitro Oocyte Culture and Somatic Cell Nuclear Transfer Used to Produce a Live-Born Cloned Goat

KATSUHIRO OHKOSHI,[1] SEIYA TAKAHASHI,[2] SHIN-ICHIRO KOYAMA,[1] SATOSHI AKAGI,[2] NORITAKA ADACHI,[2] TADASHI FURUSAWA,[1] JUN-ICHIRO FUJIMOTO,[3] KUMIKO TAKEDA,[2] MASANORI KUBO,[4] YOSHIAKI IZAIKE,[1] and TOMOYUKI TOKUNAGA[1]

ABSTRACT

The use of an *in vitro* culture system was examined for production of somatic cells suitable for nuclear transfer in the goat. Goat cumulus–oocyte complexes were incubated in tissue culture medium TCM-199 supplemented with 10% fetal bovine serum (FBS) for 20 h. *In vitro* matured (IVM) oocytes were enucleated and used as karyoplast recipients. Donor cells obtained from the anterior pituitary of an adult male were introduced into the perivitelline space of enucleated IVM oocytes and fused by an electrical pulse. Reconstituted oocytes were cultured in chemically defined medium for 9 days. Two hundred and twenty-eight oocytes (70%) were fused with donor cells. After *in vitro* culture, seven somatic cell nuclear transfer (SCNT) oocytes (3%) developed to the blastocyst stage. SCNT embryos were transferred to the oviducts of recipient females (four 8-cell embryos per female) or uterine horn (two blastocysts per female). One male clone (NT1) was produced at day 153 from an SCNT blastocyst and died 16 days after birth. This study demonstrates that nuclear transferred goat oocytes produced using an *in vitro* culture system could develop to term and that donor anterior pituitary cells have the developmental potential to produce term offspring. In this study, it suggested that the artificial control of endocrine system in domestic animal might become possible by the genetic modification to anterior pituitary cells.

INTRODUCTION

PRIOR TO 1997, DNA microinjection was the principal method used to produce transgenic farm animals (Hammer et al., 1985; Palmiter et al., 1982). While embryonic stem (ES) cells and gene-targeting techniques were effectively used to produce transgenic mice, availability of germline-competent ES cells in farm animal species proved problematic (Capecchi, 1989; Evans and Kaufman, 1981). Following the reports of nuclear transfer derived cloned sheep (Wilmut, et al., 1997), modeling efforts in a number of farm animal species focused on somatic cell nuclear transfer (SCNT) as a means of generating genetically modified farm animals efficiently. Cloned offspring have

[1]Developmental Biology Department, National Institute of Agrobiological Sciences, Ibaraki, Japan.
[2]Department of Animal Breeding and Reproduction, National Institute of Livestock and Grassland Science, Ibaraki, Japan.
[3]National Research Institute for Child Health and Development, Tokyo, Japan.
[4]National Institute of Animal Health, Ibaraki, Japan.

since been produced in other species, including mice (Wakayama et al., 1998), cattle (Cibelli et al., 2000; Kato et al., 1998), goats (Baguisi et al., 1999; Keefer et al., 2001; Reggio et al., 2001; Zou et al., 2001), swine (Onishi et al., 2000; Polejaeva et al., 2000), and rabbit (Chesne et al., 2002).

In comparison to DNA microinjection, SCNT techniques offer distinct advantages, including (1) transfected cells can be selected *in vitro* by adding a drug-resistant marker gene or reporter gene (Keefer et al., 2001; Piedrahita et al., 2000; Schnieke et al., 1997; Zou et al., 2002), (2) gene-targeting procedures can be applied to insert or delete specific genes (Denning et al., 2001), (3) generation times can be shortened by direct production of offspring derived from transfected cells, and (4) recipient females can be used more economically.

Our goal is the development of a method for artificial control of endocrine functions *in vivo* using transgenic livestock. Since the anterior pituitary (AP) is a master controller in the endocrine system *in vivo*, AP cells should be useful as SCNT donor cells in the development of this model. *In vitro* techniques and SCNT permit the genetic modification and screening of suitable donor cells for phenotypic effects of these modifications.

Here, we examined the developmental ability of SCNT oocytes derived from non-transfected cultured anterior pituitary cells.

MATERIALS AND METHODS

In vitro maturation of goat oocytes

Ovaries were harvested at slaughter from 38 Saanen female goats (kindly donated by the Shibayagi Co., Ltd.). The ovaries were maintained in 0.9% saline for 3–4 h, at which time cumulus–oocyte complexes (COCs) were obtained from small follicles (2–5 mm). COCs were then cultured in TCM-199 (Gibco, 31100-035) supplemented with 0.4 AU/mL FSH (Antorin, Denka Seiyaku), 2 μg/mL estradiol-17-β (Sigma, E-8875), 0.05 mg/mL Na pyruvate (Sigma, St. Louis, MO; P-2256), 26.2 mM $NaHCO_3$ (Nakarai, 312-13), antibiotics (penicillin + streptomycin), and 10% heat-inactivated fetal bovine serum (FBS, Tissue Culture Biologicals, 10086-1) in 5% CO_2 in air at 38.5°C for 20 h. Cumulus cells of COCs cultured for 20 h were removed in 0.5% hyarulonidase (Sigma, H-3506) solution by repeated pipetting, after which oocytes with a first polar body were enucleated for nuclear transfer.

Somatic cell nuclear transfer

Donor cells were obtained from an anterior pituitary that was extracted from a 3-month-old Japanese native (Shiba) male goat (Vale et al., 1972). A semi-confluent monolayer of donor AP cells was cultured in DMEM (Sigma, D-9756) with 0.5% FBS for the starvation. After 5–6 days of culture, donor AP cells were collected by treatment with 0.1% trypsin-EDTA.

IVM Saanen oocytes were enucleated using a micromanipulator (Narishige) and used as Shiba nuclei recipients. Karyoplasts were stained with Hoechst 33342 dye (089-03591, Wako, Japan) to confirm the success of enucleation. One donor cell was introduced into the perivitelline space of a recipient oocyte and then fused with an electric pulse of 20 V for 10 μsec in Zimmerman's cell fusion medium (Wolfe and Kraemer, 1992). After fusion stimulus, oocytes were cultured in TCM-199 medium supplemented with 10 μg/mL cycloheximide and 2.5 μg/mL cytochalasin D for 1 h, and then cultured with 10 μg/mL cycloheximide for 4 h to induce chemically activation. Fused somatic cell nuclear transfer (SCNT) oocytes were cultured in IVD-101 (Research Institute of the Functional Peptides, Japan; Abe et al., 1999) at 38.5°C in 5% CO_2, 5% O_2, 90% N_2 for 2 or 8 days. Half of the medium was changed every 2 days.

Embryo transfer and induction of parturition

Some SCNT embryos were transferred at the 2–8-cell stage (2-day culture, transfer to a recipient's oviduct) or at the blastocyst stage (8-day culture, transfer to uterus). Before embryo transfer, estrus cycles of recipient females were synchronized by two injections of 15 and 10 mg prostaglandin F2α (PGF2α, Panaseran Hi, Daiichi Seiyaku) at 12-h intervals. Prior to laparotomy, females were anesthetized with ketamine hydrochloride (2 mg/kg, Ketararu, Sankyo) and xylazine hydrochloride (0.5 mg/kg, Serakutaru, Bayer). The oviduct or uterine horn was exteriorized through a midline laparotomy, and the SCNT embryos were introduced into the oviduct or uterine horn. Before closure, to prevent abdominal adhesion, 5 mL of a solution of 1% condroitin mono sulfate (condoron, Kaken Seiyaku Co., Ltd) was dripped into the peritoneal cavity.

TABLE 1. *IN VITRO* DEVELOPMENT OF SOMATIC CELL NUCLEAR TRANSFERRED OOCYTES[a]

	Development of fused oocytes (%)				*No. of embryos transferred*	
No. of oocytes fused/total (%)	*2-cell*	*4-cell*	*8-cell*	*Blastocyst*	*Oviduct (4- to 8-cell stage ova)*	*Uterus (blastocysts)*
228/325 (70)	109 (48)	86 (38)	24 (11)	7 (3)	4	2

[a]Somatic cell nuclei derived from adult goat pituitary cells.

After closure, antibiotics (Ampicillin, Mitaka Seiyaku Co., Ltd.) were given to the recipient by injection IM. Pregnancy was monitored with an ultrasound instrument (EUB-405, HitachiMedico) every 10th day starting at day 35.

Parturition was induced by serial injections of 12.5 mg PGF2α at day 152, following an injection of 10 mg dexamethasone and 12.5 mg PGF2α on day 151.

Genotype analysis of cloned kid

In order to confirm the genotypes of donor cells, cloned kid (NT1) and recipient/control goats, nested PCR analysis of the MHC class II DRB region was performed using the method of Amills et al. (1996). Genomic DNA was extracted from donor cells, and blood samples were taken from the cloned kid and other goats using the DNeasy Tissue Kit (Qiagen). For the first PCR of the MHC class II DRB region, primers DRB1-1 (5′-TATCCCGTCTCTGCAGCACATTTC-3′) and Gio (5′-CGTACCCAGAGTGAGTGAAGTATC-3′) were used. The amplification was performed in a 25-μL reaction volume containing 100 ng of each template DNA, 1 pmol of each primer, 1 × PCR buffer, 0.2 mM dNTPs, and 0.2 unit of Taq DNA polymerase (AmpliTaq, Roche Diagnostics GmbH, Mannheim, Germany). The reactions were incubated in a thermal cycler (Gene Amp PCR system 9700; PE Biosystems) under the following conditions: 95°C for 1 min for first denaturing, 10 cycles of 94°C for 30 sec, 55°C for 1 min, and 72°C for 1 min. For the second PCR, primers DRB1-1 and DRB1-2 (5′-TCGCCGCTGCACACTGAAACTCTC-3′) were used. The amplification was performed in a 25-μL reaction volume containing 5 μL of each of the first-PCR products, 1 pmol of each primer, 1 × PCR buffer, 0.2 mM dNTP, and 0.2 unit of Taq DNA polymerase. The reactions were amplified under the following conditions: 95°C for 1 min for first denaturing, 30 cycles of

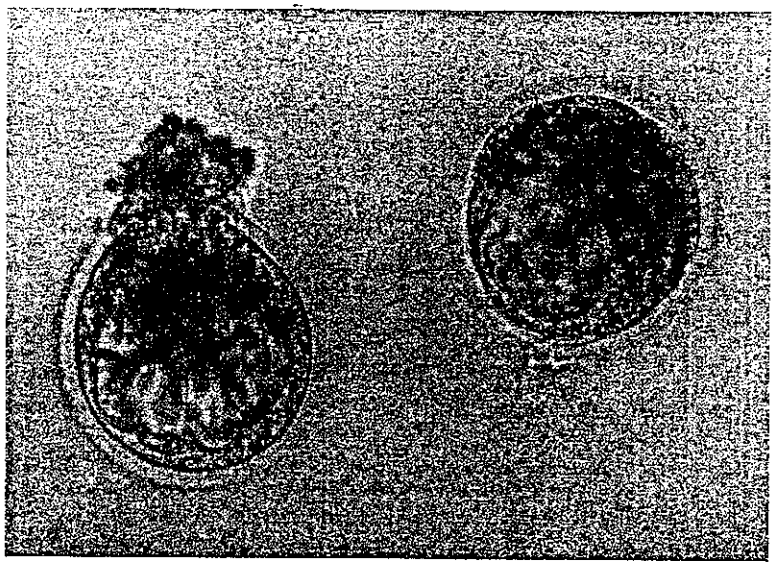

FIG. 1. Representative somatic cell nuclear transfer blastocyst at the time of transfer to the uterine horn of a recipient female. Note normal morphological appearance of expanded/hatching blastocysts.

94°C for 30 sec, 62°C for 1 min, and 72°C for 1 min. Second-round amplification products were digested overnight with the restriction enzyme *Rsa*I at 37°C and separated on a 10% polyacrylamide gel before visualization. The resulting band patterns were visualized by silver staining (Silver Stain Kit, Wako, Japan).

In order to confirm a recipient–kid mismatch (no genetic relationship), mtDNA genotypes were determined by PCR-mediated single-strand conformation polymorphism (SSCP) analysis as described by Takeda et al. (1995). PCR primers were designed from the reported sequences of goat mtDNA (Takada et al., 1997) targeted to the displacement (D)–loop region DL-F (5′-CACACGTATAAAAACATCCCAATC-3′) and DL-R (5′-ACCATGTAAAAGACCCAGGCAC-3′). The amplification was performed in a 25-μL reaction volume containing 12.5 pmol of each primer, 1 × PCR buffer, 0.2 mM dNTPs, and 1 unit of Fast Start Taq DNA polymerase (Roche Diagnostics GmbH, Mannheim, Germany). The reactions were amplified under the following conditions: 95°C for 4 min for first denaturing, 35 cycles of 95°C for 30 sec, 60°C for 30 sec, 72°C for 2 min, and 72°C for 4 min for final extension. PCR products were digested by restriction enzyme *Bst*UI or *Hinf*I. For SSCP analysis, samples were analyzed on 6% polyacrylamide containing 5% glycerol. Electrophoresis was performed in 0.5 × TBE buffer at 120 V for 4 h at 4°C. The resulting band patterns were visualized by silver staining (Silver Stain Plus Kit, Bio Rad Laboratory, Hercules, CA).

RESULTS

Somatic cell nuclear transfer

As shown in Table 1, the developmental rates of SCNT oocytes receiving adult AP cells were low (3%, 7/228). Four SCNT 2–8-cell embryos or two SCNT blastocysts were transferred to oviduct or uterus of each recipient female (Fig. 1). Pregnancy of the recipient with transplanted blastocysts was confirmed at day 35. Labor was initiated 26 h after PGF2α injection, and one male cloned kid (NT1) was born at 28 h post-PGF2α (Fig. 2). His birth weight was 1.25 kg.

FIG. 2. Cloned Shiba kid (NT1) and recipient Shiba female (N9).

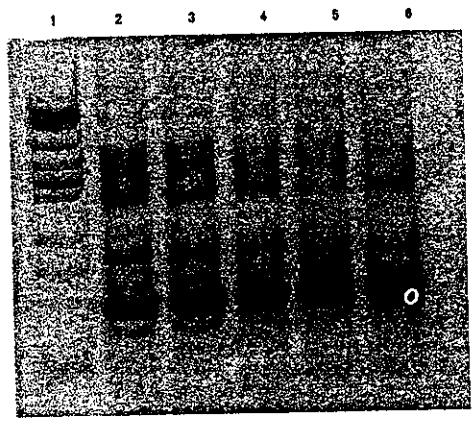

FIG. 3. Electrophoretic separation of the nested PCR products of MHC class II DRB DNA treated with Ras I. Lane 1, marker ϕ 174 Hinc III. DNA samples: Lane 2, DNA from cloned kid (NT1). Lane 3, donor cells. Lane 4, recipient female (N9). Lane 5, control female (Z16). Lane 6, control male offspring of control female (N16).

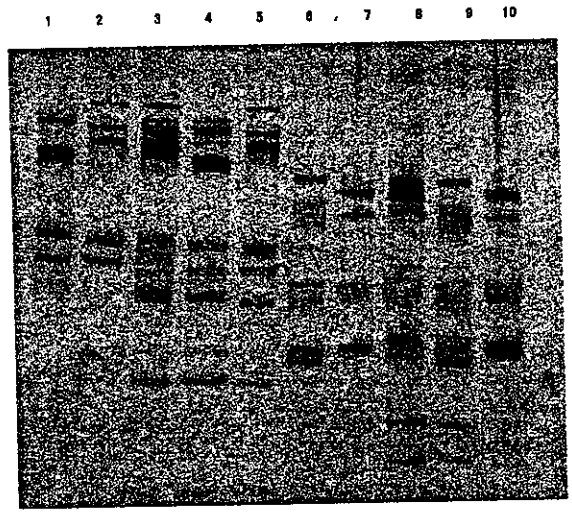

FIG. 4. Electrophoretic separation of PCR amplified mtDNA. The mtDNA D-loop region was amplified and separated on silver-stained 6% gel. Lanes 1–5, PCR products digested with BstUI; Lanes 6–10, PCR products digested with HinfI. Lanes 1 and 6, recipient female N9. Lanes 2 and 7, control female Z16. Lanes 3 and 8, cloned kid NT1. Lanes 4 and 9, donor cell clone sample. Lanes 5 and 10, control male offspring of female Z16.

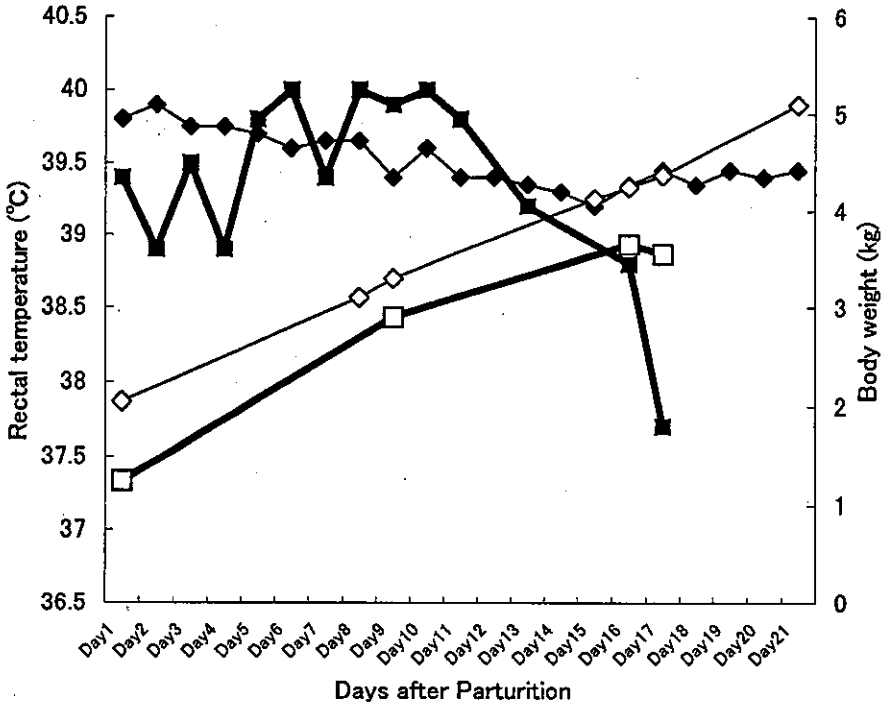

FIG. 5. Change of body weight and rectal temperature of male clone (NT1) and controls. ■, Body weight of NT kid; □, rectal temperature of NT kid; ◆, means of male body weight; ◇, means of male rectal temperature.

Analysis of MHC class II DRB and mt DNA genotypes

Nested PCR analysis of MHC class II DRB region confirmed that the genome of the cloned kid was identical to that of the donor cells (Fig. 3). However, the cloned kid also had a pattern similar to, but distinct from that of the recipient female. Investigation revealed that the donor male Shiba goat was actually related to the recipient female goat. However, the results of PCR-mediated SSCP analysis effectively confirmed that the mtDNA genotype of the cloned kid was different from the mtDNA of both of the recipient female and donor cell (Fig. 4).

Growth and death of cloned kid

Initially, the cloned kid developed normal postnatally (Fig. 5). However, he suddenly died 16 days after a detected decrease in body temperature. A necropsy was performed immediately after death, where it was observed that the kid suffered from umbilical cord pathology (insufficiency of involution of the umbilical cord vein) and abnormal liver pathology. For the histological tissue examination, tissues from the liver, spleen, kidney, heart, lung, thymus, trachea, digestive organs, lymph nodes, bladder, testis, brain, and bone marrow was collected. Within collected organ, there was any histologi-

TABLE 2. POSTMORTEM ANALYSIS OF TISSUES FROM CLONED KID THAT DIED AT 16 DAYS OLD

Organ	*Pathology view*
Liver	Hyperplasia of connective tissues, glass-like degeneration of hepatic cell, ectopic hematopoiesis, enlarged capsule
Kidney	Ectopic hematopoiesis, fatty degeneration in epithelium of tubulus renalis
Spleen	Enlarged follicles
Lung	Ectopic hematopoiesis in granulocytes
Heart	Glass-like degeneration, proliferation of interstitial cells
Lymph nodes	Ectopic hematopoiesis
Bladder	Calcification of artery
Testis	Ectopic hematopoiesis in connective tissues

cal abnormality in eight organs (Table 2). The most abounding abnormality was an ectopic hematopoiesis, and it was observed in liver, kidney, lung, lymph node, and testis. And the glass-like degeneration was observed in hepatic cell and myocardium. As other abnormalities, hyperplasia of connective tissues and enlarged capsule in liver, fatty degeneration in epithelium of tubulus renalis, enlarged follicles in spleen, and calcification of artery in bladder were observed.

DISCUSSION

In this study, we produced a nuclear transfer–derived cloned goat using an *in vitro* culture system. Recipient oocytes were matured *in vitro*, and SCNT oocytes then were cultured *in vitro* through the blastocyst stage. Two-cell to blastocyst stage ova were transferred to recipient females for the remainder of gestation. To our knowledge, this is the first report of IVC-derived SCNT blastocysts to term in the goat.

The SCNT-derived kid was confirmed by MHC class II DRB RFLP. However, since the male goat that provided the donor cell was distantly related to the recipient female, initially it was difficult to show a difference between the cloned kid and the recipient female. However, based on maternal mitochondrial inheritance, analysis of mtDNA was performed and provided confirmation that the cloned kid was derived by SCNT. The results indicated that the mtDNA of the cloned kid differed from that of both the recipient female and the donor cell. These data proved that the goat kid produced in this study was a clone of cultured anterior pituitary cells. They also confirmed previous observations that suggested that the mitochondria of cloned animals are derived not from donor cells but from recipient oocytes (Evans et al., 1999; Takeda et al., 1999).

Birth weight of cloned kid was 1.25 kg, which is not significantly different from the means of Shiba male goat (1.65 kg) in our laboratory. This may be because the defined culture medium, IVD-101, used in this study did not contain serum (Thompson et al., 1995). The growth rate of clone was the same as that of control kids. However, there was an intense change in the rectal temperature of the clone compared to the normal kids (Fig. 5). After the onset of hypothermia at 16 days of age (37.7°C), the cloned kid died. Necropsy results revealed that insufficiency of involution of the umbilical cord vein, an abnormal form of liver and that the blood become whitely impure. These abnormalities, in particular that of the liver, were reported in bovine SCNT offspring (Hill et al., 1999; Kubo, 2002). In addition, ectopic hematopoiesis in the liver, kidney, spleen, and lung was observed in the histological sections.

In this study, we have demonstrated that AP-derived SCNT goat embryos, produced using an *in vitro* culture system, have the developmental potential to progress to term. The SCNT system that we have developed should be effective in the production of the transgenic goat. Genetically modified AP cells will be screened *in vitro* to determine the effects of the transgene prior to SCNT, thus increasing the chance of obtaining the desired phenotype in the transgenic SCNT-derived goats. Although we are currently forcing the reduction of growth hormone secretion using antisense technology as a model for genetically modified livestock, further studies will be needed to improve SCNT before production of such genetically modified animals can be achieved at reasonable efficiencies.

ACKNOWLEDGMENTS

We thank Dr. Carl A. Pinkert for comments and critical discussion of this manuscript. This study was granted by Organized Research Combination System, M.E.X.T., Japan. Special thanks go to NLBC (Nagano Station), Shibayagi Co., Ltd., and Nippon Zenyaku Kogyo Co., Ltd. for their support.

REFERENCES

Abe, H., Yamashita, S., Itoh, T., et al. (1999). Ultrastructure of bovine embryos developed from *in vitro*–matured and –fertilized oocytes: comparative morphological evaluation of embryos cultured either in serum-free medium or in serum-supplemented medium. Mol. Reprod. Dev. 53, 325–335.

Amills, M., Francino, O., and Sanchez, A. (1996). A PCR-RFLP typing method for the caprine Mhc class II DRB gene. Vet. Immunol. Immunopathol. 55, 255–260.

Baguisi, A., Behboodi, E., Melican, D.T., et al. (1999). Production of goats by somatic cell nuclear transfer. Nat. Biotechnol. 17, 456–461.

Capecchi, M.R. (1989). Altering the genome by homologous recombination. Science 244, 1288–1292.

Chesne, P., Adenot, P.G., Viglietta, C., et al. (2002). Cloned rabbits produced by nuclear transfer from adult somatic cell. Nat. Biotechnol. 20, 366–369.

Cibelli, J.B., Stice, S.L., Golueke, P.J., et al. (2000). Cloned transgenic calves produced from nonquiescent fetal fibroblasts. Science 280, 1256–1258.

Denning, C., Burl, S., Ainslie, A., et al. (2001). Deletion of the α-(1,3)-galactosyl transferase (GGTA1) gene and the prion protein (PrP) gene in sheep. Nat. Biotechnol. 19, 559–562.

Evans, M.J., and Kaufman, K.H. (1981). Establishment in culture of pluripotent cells from mouse embryos. Nature 292, 154–156.

Evans, M.J., Gurer, C., Loike, J.D., et al. (1999). Mitochondrial DNA genotype in nuclear transfer-derived cloned sheep. Nat. Genet. 23, 90–93.

Hammer, R.E., Pursel, V.G., Rexroad, Jr., C.E., et al. (1985). Production of transgenic rabbits, sheep and pigs by microinjection. Nature 315, 680–683.

Hill, J.R., Roussel, A.J., Cibelli, J.B., et al. (1999). Clinical and pathologic features of cloned transgenic calves and fetuses (13 case studies). Theriogenology 51, 1451–1465.

Kato, Y., Tani, T., Sotomaru, Y., et al. (1998). Eight calves cloned from somatic cells of a single adult. Science 282, 2095–2097.

Keefer, C.L., Baldassarre, H., Keyston, R., et al. (2001). Generation of dwarf goat (*Capra hircus*) clones following nuclear transfer with transfected and nontransfected fetal fibroblasts and *in vitro*–matured oocytes. Biol. Reprod. 64, 849–856.

Kubo, M. (2002). Pathology of diseases in calves cloned by nuclear transfer. Cloning Stem Cells 4, 281(abstr).

Onishi, A., Iwamoto, M., Akita, T., et al. (2000). Pig cloning by microinjection of fetal fibroblast nuclei. Science 289, 1188–1190.

Palmiter, R.D., Brinster, R.L., Hammer, R.E., et al. (1982). Dramatic growth of mice that develop from eggs microinjected with metallothionein–growth hormone fusion genes. Nature 300, 611–615.

Piedrahita, J.A. (2000). Targeted modification of the domestic animal genome. Theriogenology 53, 105–116.

Polejaeva, I., Chen, S.H., Vaught, T.D., et al. (2000). Cloned pigs produced by nuclear transfer from adult somatic cells. Nature 407, 505–509.

Reggio, B.C., James, A.N., Green, H.L., et al. (2001). Cloned transgenic offspring resulting from somatic cell nuclear transfer in the goat: oocytes derived from both follicle-stimulating hormone-stimulated and nonstimulated abattoir-derived ovaries. Biol. Reprod. 65, 1528–1533.

Schnieke, A.E., Kind, A.J., Ritchie, W.A., et al. (1997). Human factor IX transgenic sheep produced by transfer of nuclei from transfected fetal fibroblasts. Science 278, 2130–2133.

Takada, T., Kikkawa, Y., Yonekawa, H., et al. (1997). Bezoar (*Capra aegagrus*) is a matriarchal candidate for ancestor of domestic goat (*Capra hircus*): evidence from the mitochondrial DNA diversity. Biochem. Genet. 35, 315–326.

Takeda, K., Onishi, A., Ishida, N., et al. (1995). SSCP analysis of pig mitochondrial DNA D-loop region polymorphism. Anim. Genet. 26, 321–326.

Takeda, K., Takahashi, S., Onishi, A., et al. (1999). Dominant distribution of mitochondrial DNA from recipient oocytes in bovine embryos and offspring after nuclear transfer. J. Reprod. Fertil. 116, 253–259.

Thompson, J.G., Gardner, D.K., Pugh, P.A., et al. (1995). Lamb birth weight is affected by culture system utilized during *in vitro* pre-elongation development of ovine embryos. Biol. Reprod. 53, 1385–1391.

Vale, W., Grant, G., Amoss, M., et al. (1972). Culture of enzymatically dispersed anterior pituitary cells: functional validation of a mothod. Endocrinology 91, 562–572.

Wakayama, T., Perry, A.C.F., Zucotti, M., et al. (1998). Full-term development of mice from enucleated oocytes injected with cumulus cell nuclei. Nature 394, 369–374.

Wilmut, I., Schnieke, A.E., McWhir, J., et al. (1997). Viable offspring derived from fetal and adult mammalian cell. Nature 385, 810–813.

Wolfe, B.A., and Kraemer, D.C. (1992). Methods in bovine nuclear transfer. Theriogenology 37, 5–15.

Zou, X., Chen, Y., Wnag, Y., et al. (2001). Production of cloned goats from enucleated oocytes injected with cumulus cell nuclei or fused with cumulus cells. Cloning 3, 31–37.

Zou, X., Wang, Y., Cheng, Y., et al. (2002). Generation of cloned goats (*Capra hircus*) from transfected foetal fibroblast cells, the effect of donor cell cycle. Mol. Reprod. Dev. 61, 164–172.

Address reprint requests to:
Tomoyuki Tokunaga
Department of Developmental Biology
National Institute of Agrobiological Sciences
2 Ikenodai, Tsukuba
Ibaraki 305-8602, Japan

E-mail: tom@affrc.go.jp

nature
cell biology

Mechanical stress activates angiotensin II type 1 receptor without the involvement of angiotensin II

Yunzeng Zou[1], Hiroshi Akazawa[1], Yingjie Qin[1], Masanori Sano[1], Hiroyuki Takano[1], Tohru Minamino[1], Noriko Makita[2], Koji Iwanaga[1], Weidong Zhu[1], Sumiyo Kudoh[3], Haruhiro Toko[1], Koichi Tamura[4], Minoru Kihara[4], Toshio Nagai[1], Akiyoshi Fukamizu[5], Satoshi Umemura[4], Taroh Iiri[2], Toshiro Fujita[2] and Issei Komuro[1,6]

The angiotensin II type 1 (AT1) receptor has a crucial role in load-induced cardiac hypertrophy. Here we show that the AT1 receptor can be activated by mechanical stress through an angiotensin-II-independent mechanism. Without the involvement of angiotensin II, mechanical stress not only activates extracellular-signal-regulated kinases and increases phosphoinositide production *in vitro*, but also induces cardiac hypertrophy *in vivo*. Mechanical stretch induces association of the AT1 receptor with Janus kinase 2, and translocation of G proteins into the cytosol. All of these events are inhibited by the AT1 receptor blocker candesartan. Thus, mechanical stress activates AT1 receptor independently of angiotensin II, and this activation can be inhibited by an inverse agonist of the AT1 receptor.

Cardiac hypertrophy is not only an adaptational state before cardiac failure, but also an independent risk factor of major cardiac events[1]. It is thus very important to understand the molecular mechanism that underlies the development of cardiac hypertrophy. Although various humoral factors such as vasoactive peptides, catecholamines, cytokines and growth factors can contribute to the development of cardiac hypertrophy during the increase in haemodynamic load, the initial stimulus mechanical stress is the most important contributory factor[2].

To dissect the mechanism of how mechanical stress induces cardiac hypertrophy, we and others have developed an *in vitro* device by which stretch stimuli can be imposed on cultured cardiomyocytes[3,4]. Mechanical stretch induces the activation of many protein kinases including extracellular-signal-regulated kinases (ERKs), reprogramming of gene expression, and cardiomyocyte hypertrophy in cultured cardiomyocytes[5]. Pretreatment of cardiomyocytes with angiotensin II (AII) type (AT1) receptor blockers significantly attenuates all of these mechanical-stretch-induced events[6,7]. Furthermore, many animal and clinical studies have shown that AT1 receptor blockers induce regression of cardiac hypertrophy and prevent progression of heart failure, resulting in a reduction in cardiac morbidity and mortality[8–12].

These basic and clinical studies have suggested that the local renin–angiotensin system (RAS) is activated by haemodynamic overload and that the AT1 receptor has a crucial role in the development of load-induced cardiac hypertrophy; however, it remains unclear how the AT1 receptor is activated by mechanical stress. It has been reported that AII is stored in cardiomyocytes and that mechanical stretch induces the secretion of stored AII into the culture medium, resulting in the induction of cardiomyocyte hypertrophy by the autocrine mechanism[6]. Here we have examined the possibility that mechanical stress can directly activate the AT1 receptor without the involvement of AII.

RESULTS

Marginal roles of endogenous AII in cardiomyoctes

Mechanically stretching cardiomyocytes by 20% for 8 min activated ERKs, and this activation was significantly inhibited by an AT1 receptor blocker, candesartan, as reported previously[7] (Fig. 1a, lanes 2 and 4). The magnitude of the stretch-induced activation of ERKs was the same as that induced by exposing the cardiomyocytes to 10^{-8} to 10^{-7} M AII (Fig. 1a, lanes 7, 8). These results indicate that the AT1 receptor is crucially involved in the stretch-induced activation of ERKs in cardiomyocytes and suggest that AII is secreted from cardiomyocytes into the culture medium by stretch.

We first used radioimmunoassay to measure AII in culture medium conditioned by stretching cardiomyocytes for 8 min, but did not detect a significant increase in AII concentration after stretch (AII without stretch, $0.7 \pm 1.6 \times 10^{-12}$ M; AII with stretch, $2.0 \pm 3.5 \times 10^{-12}$ M; not significant; Fig. 1b). We then carried out a bioassay using human embryonic kidney 293 cells expressing the

[1]Department of Cardiovascular Science and Medicine, Chiba University Graduate School of Medicine, 1-8-1 Inohana, Chuo-ku, Chiba 260-8670, Japan. [2]Department of Nephrology and Endocrinology, University of Tokyo Graduate School of Medicine, 7-3-1 Hongo, Bunkyo-ku, Tokyo 113-8655, Japan. [3]Department of Cardiology, Kanazawa Medical University, 1-1 Daigaku, Uchinada-cho, Kawakita, Ishikawa 920-0265, Japan. [4]Department of Internal Medicine II, Yokohama City University School of Medicine, 3-9 Fukuura, Kanazawa-ku, Yokohama, Kanagawa 236-0004, Japan. [5]Center for Tsukuba Advanced Research Alliance, Institute of Applied Biochemistry, University of Tsukuba, Tennoudai 1-1-1, Tsukuba, Ibaraki 305-8577, Japan.
[6]Correspondence should be addressed to I.K. (e-mail: komuro-tky@umin.ac.jp)

Published online: 16 May 2004; DOI:10.1038/ncb1137

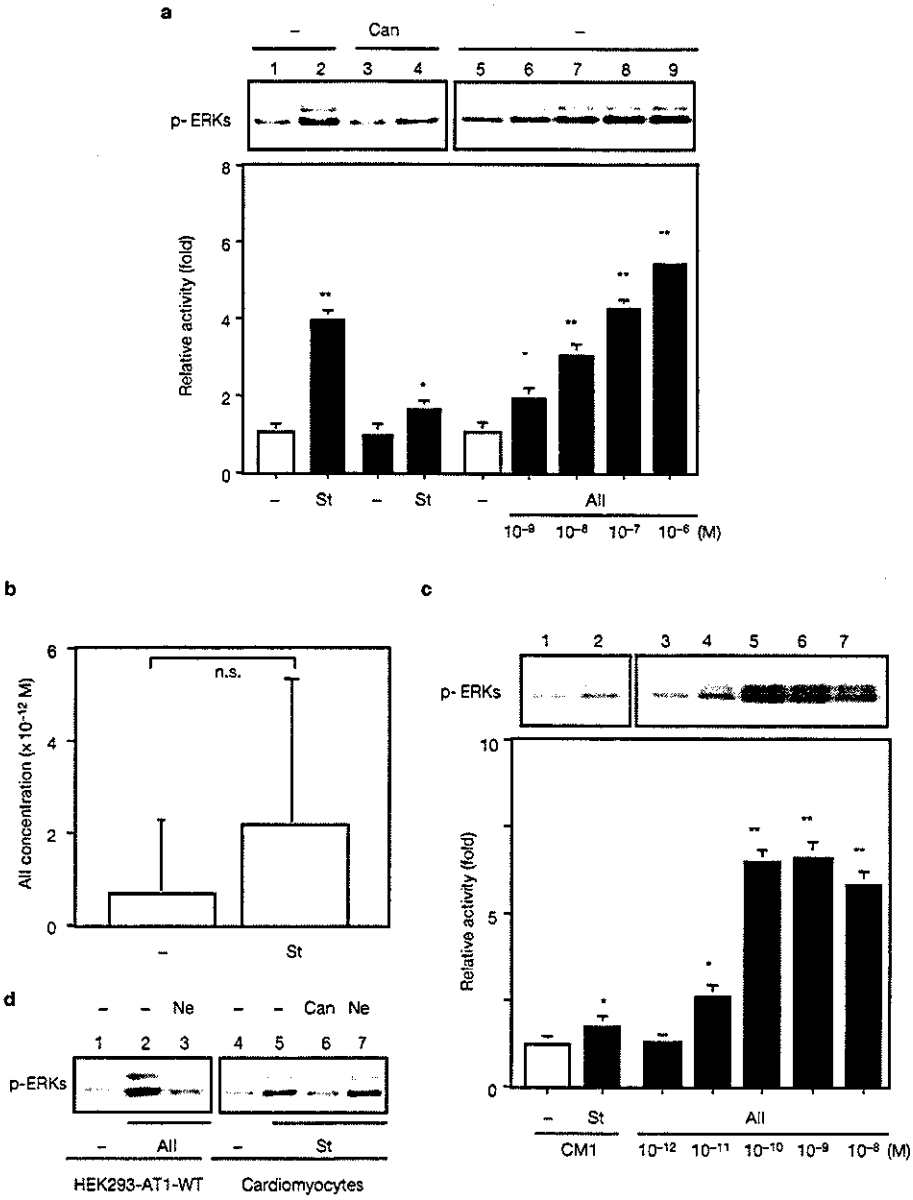

Figure 1 Activation of ERKs by mechanical stretch, AII and conditioned medium. (a) Cultured cardiomyocytes of neonatal rats were pretreated with 10^{-7} M candesartan (Can) or vehicle (–), and either stretched by 20% (St) or incubated with the indicated concentrations of AII for 8 min. Activation of ERKs was determined by using antibodies against phosphorylated ERKs (p-ERKs). The relative kinase activities of an ERK of relative molecular mass 42,000 (M_r 42K) were determined by scanning each band with a densitometer. Results are shown as the fold increase in activity over unstimulated cells and are the mean ± s.e.m. of three independent experiments. $^*P < 0.05$, $^{**}P < 0.01$ versus vehicle. (b) The culture medium from cardiomyocytes conditioned by stretch (St) or no stretch (–) was measured for AII by radioimmunoassay. Results are the mean ± s.e.m. of six samples. n.s., not significant. (c) HEK293-AT1-WT cells were exposed to conditioned medium collected before (–) or after stretching (St) cardiomyocytes for 8 min (CM1) or to the indicated concentrations of AII. Relative kinase activities of the 42K ERK were determined as in a. $^*P < 0.05$, $^{**}P < 0.01$, as compared with vehicle. (d) HEK293-AT1-WT cells or cardiomyocytes were subjected to AII or stretch for 8 min without (–) or with (Ne) the presence of a neutralizing antibody to AII (10 μg ml^{-1}; Cortex Biochem).

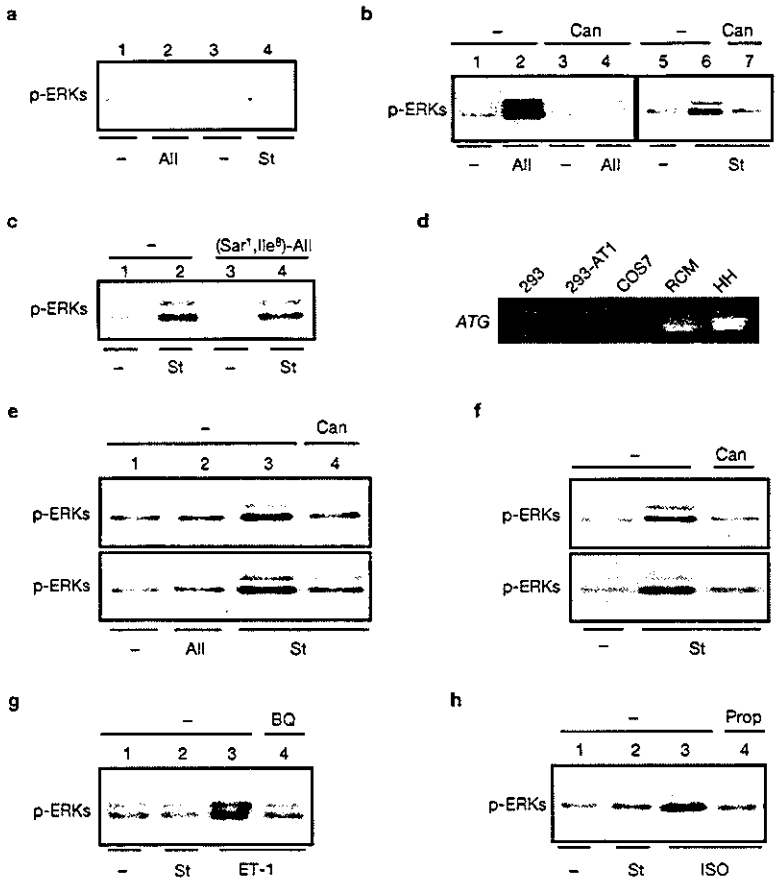

Figure 2 AII-independent activation of ERKs by mechanical stretch in cells overexpressing AT1 receptors. (a) HEK293 cells were stretched by 20% (St) or exposed to 10^{-7} M AII for 8 min. (b) HEK293-AT1-WT cells were stimulated by mechanical stretch or AII in the absence (–) or presence of 10^{-7} M candesartan (Can). (c) HEK293-AT1-WT cells were stretched in the absence (–) or presence of 10^{-7} M (Sar^1,Ile^8)-AII. (d) Expression of the *ATG* gene analysed by RT–PCR. 293, HEK293 cells; 293-AT1, HEK293-AT1-WT cells; RCM, cardiomyocytes of neonatal rats; HH, human heart. (e) HEK293 (top) and COS7 cells (bottom) were transiently transfected with AT1-mut1, which does not bind to AII. Cells were stimulated with mechanical stretch or AII without (–) or with candesartan (Can). (f) Cardiomyocytes prepared from neonatal (top) and adult (bottom) *ATG*$^{-/-}$ mice were pretreated with candesartan, and then stimulated with mechanical stretch. (g, h) COS7 cells transiently transfected with ET1A (g) or β2-AR (h) receptors were pretreated with an ET1A antagonist BQ123 (BQ), a β-AR blocker propranolol (Prop) or vehicle (–), and then stimulated with mechanical stretch, ET-1 or ISO.

wild-type mouse AT1a receptor (hereafter denoted HEK293-AT1-WT cells). The medium conditioned by stretching cardiomyocytes for 8 min only slightly activated ERKs in HEK293-AT1-WT cells (Fig. 1c, lane 2). Its activity was equivalent to that induced by incubating HEK293-AT1-WT cells with 10^{-12} to 10^{-11} M AII (Fig. 1c, lanes 3 and 4), a value that was similar to the concentration of AII measured in the medium by radioimmunoassay. These results suggest that AII, even if secreted, would not be enough to induce the full activation of the AT1 receptor observed after stretch.

To confirm whether secreted AII has a marginal role in the stretch-induced activation of ERKs, we blocked AII activity with a neutralizing antibody to AII. Although the antibody abolished the activation of ERKs induced by 10^{-7} M AII (Fig. 1d, lane 3), it did not significantly suppress the stretch-induced activation of ERKs (Fig. 1d, lane 7).

Stretch activates ERKs through the AT1 receptor without AII

Neither mechanical stretch nor AII (10^{-7} M) activated ERKs in HEK293 cells (Fig. 2a). In HEK293-AT1-WT cells, however, both mechanical stretch and AII activated ERKs (Fig. 2b, lanes 2 and 6). Pretreatment with the AT1 receptor blocker candesartan inhibited the activation of ERKs induced not only by AII (Fig. 2b, lane 4) but also by mechanical stretch in HEK293-AT1-WT cells (Fig. 2b, lane 7). Basal ERK activity was also decreased by candesartan (Fig. 2b, lane 3) in HEK293-AT1-WT cells, and similar results were obtained in COS7 cells transiently expressing AT1-WT.

Mechanical stretch activated ERKs in COS7 cells expressing AT1-WT (see Supplementary Information Fig. S1) but not in COS7 cells (data not shown). Candesartan also reduced the basal and the stretch-enhanced ERK activities in these cells (see Supplementary Information Fig. S1). However, a competitive inhibitor for AII, (Sar^1,Ile^8)-AII, did

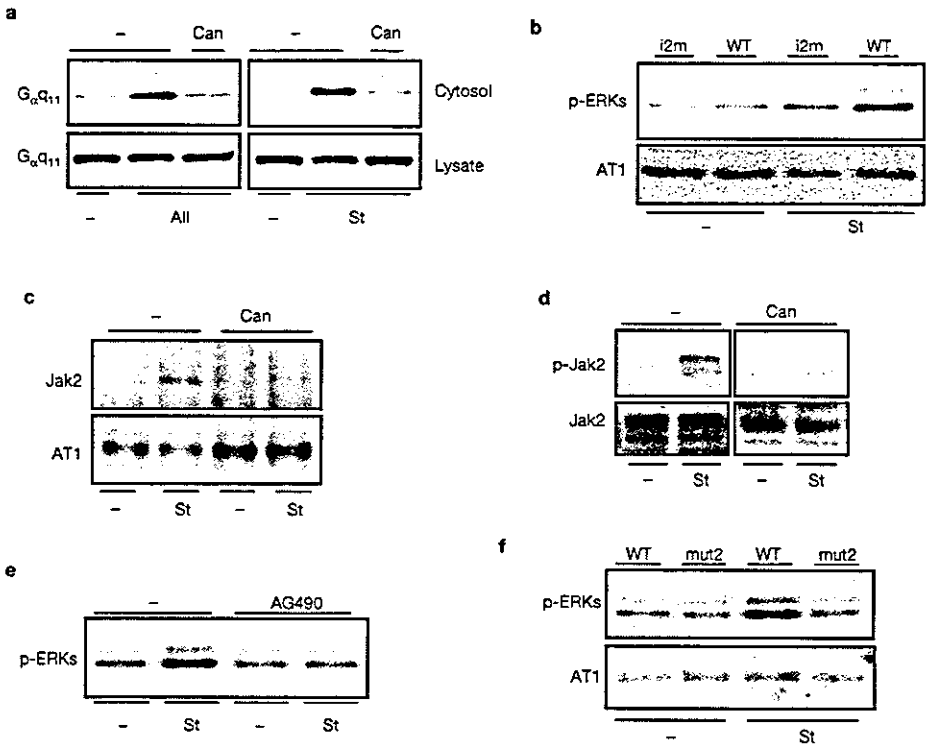

Figure 3 Activation of G proteins and Jak2 by mechanical stretch, and their effects on ERK activation. (a) HEK293T-AT1-WT cells, pretreated with candesartan (Can) or vehicle (–), were stimulated with AII or mechanical stretch (St) for 5 min. Aliquots of the cytosol (top) and whole lysates (bottom) were resolved by SDS–PAGE. Blotted membranes were incubated with an antibodies against $G_\alpha q_{11}$. (b) COS7 cells were transfected with AT1-i2m (i2m), which lacks a binding domain for G proteins, or the wild-type AT1 receptor (WT), and stretched for 8 min (top). Receptor transfection was verified by an antibody against the AT1 receptor (bottom). (c) HEK293T-AT1-WT cells, pretreated with candesartan (Can) or vehicle (–), were subjected to mechanical stretch for 5 min. Total cell lysates were immunoprecipitated by an antibody against the AT1 receptor and the immunocomplexes were subjected to immunoblotting with antibodies against Jak2 (top) or the AT1 receptor (bottom). (d) HEK293T-AT1-WT cells, pretreated with candesartan (Can) or vehicle (–), were subjected to mechanical stretch. Blotted membranes were incubated with antibodies against phosphorylated Jak2 (top) or total Jak2 (bottom). (e) HEK293T-AT1-WT cells, pretreated with tyrphostin AG490 or vehicle (–), were stretched by 20% for 8 min. (f) COS7 cells were transfected with AT1-mut2 (mut2), which lacks a binding domain for Jak2, or the wild-type AT1 receptor (WT), and stimulated by mechanical stretch for 8 min (top). Receptor transfection was verified by an antibody against the AT1 receptor (bottom).

not attenuate stretch-induced ERK activation in HEK293-AT1-WT cells (Fig. 2c, lane 4), although this inhibitor abolished AII-induced ERK activation in the same cells (data not shown).

These results indicate that expression of the AT1 receptor provides HEK293 and COS7 cells with the ability to respond to stretch, for which there might be two possible mechanisms. First, AII is stored in these cells and secreted by stretch, but the cells do not respond to secreted AII because they lack the AT1 receptor. Second, the AT1 receptor is activated by stretch without the involvement of AII.

The medium conditioned by stretching HEK293-AT1-WT cells did not activate ERKs in HEK293-AT1-WT cells (see Supplementary Information Fig. S2). Analysis by polymerase chain reaction with reverse transcription (RT–PCR) did not detect the transcript of the angiotensinogen gene (*ATG*) in HEK293, COS7 or HEK293-AT1-WT cells even after 50 cycles, although it was detected in cardiomyocytes of neonatal rats and human hearts (Fig. 2d). Taken together, these results suggest that mechanical stretch activates the AT1 receptor in both HEK293-AT1-WT cells and COS7 cells expressing the AT1 receptor without the secretion of AII.

To confirm whether or not AT1 receptor is activated by mechanical stretch without involving its ligand, we stretched HEK293 and COS7 cells expressing an AT1 receptor whose binding site for AII was mutated by the replacement of Lys 199 with glutamine (AT1-mut1)[13]. AII did not activate ERKs in cells expressing AT1-mut1 (Fig. 2e, lane 2), indicating a lack of coupling between the mutated receptor and AII. In the same AT1-mut1 cells, however, ERKs were strongly activated by mechanical stretch, and this activation was inhibited by candesartan (Fig. 2e, lanes 3 and 4).

To confirm further activation of the AT1 receptor by mechanical stretch without the involvement of AII, we stretched cardiomyocytes prepared from *ATG*-deficient ($ATG^{-/-}$) mice, in which AII is not detected[14]. Mechanical stress activated ERKs in the cardiomyocytes prepared from both neonatal (Fig. 2f, top) and adult $ATG^{-/-}$ mice (Fig. 2f, bottom). Pretreatment of these cells with candesartan markedly suppressed the activation of ERKs (Fig. 2f). These results indicate that mechanical stress may activate ERKs in cardiomyocytes through the AT1 receptor even in the absence of AII.

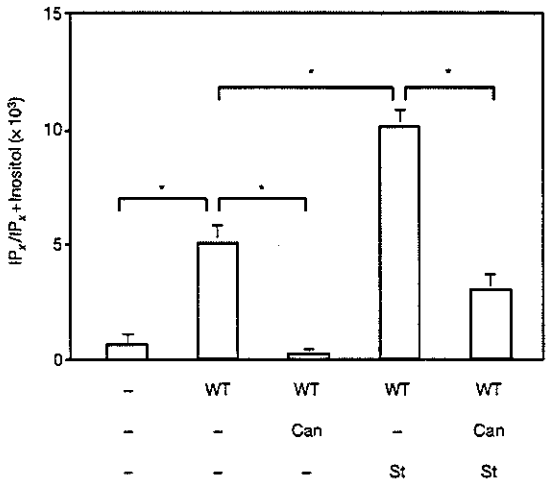

Figure 4 Mechanical-stretch-stimulated production of inositol phosphates through the AT1 receptor. COS7 cells (–) or COS7 cells transfected with AT1-WT (WT) were labelled with myo-[^{3}H]inositol 24 h after transfection. After 24 h of labelling, cells were incubated with vehicle (–) or candesartan (Can) for 5 h at 37 °C. The accumulation of inositol phosphates was measured as described in Methods. Some COS7 cells transiently transfected with AT1-WT (WT) were subjected to stretching (St) for 45 min or no stimulus (–) in the presence of 5 mM LiCl. *$P < 0.05$.

The AT1 receptor is a guanine-nucleotide-binding protein (G-protein)-coupled receptor (GPCR), a member of a large family of cell-surface receptors that contain common structural features characterized by seven transmembrane helices essential for signal transduction[15–17]. Activation of other GPCRs, such as the receptors of endothelin 1 (ET-1) and catecholamines, also induces cardiomyocyte hypertrophy[18,19]. We therefore tested whether mechanical stretch can activate these receptors in a ligand-independent manner. We stretched COS7 cells overexpressing either the wild-type ET-1 type A (ET1A) receptor (Fig. 2g) or the wild-type β2-adrenoceptor (β2-AR; Fig. 2h). Whereas ET-1 and isoproterenol (ISO) activated ERKs, mechanical stretch did not evoke significant activation of ERKs in these transfected cells. These results suggest that the activation of GPCRs by mechanical stretch without the involvement of their ligands is not a general phenomenon but specific to some GPCRs including the AT1 receptor.

G proteins and Jak2 are activated by stretch

As a member of the GPCR family, the AT1 receptor evokes intracellular signals through G proteins[20,21]. We therefore examined whether mechanical stress could activate G proteins through the AT1 receptor. Stimulation with either AII or mechanical stretch induced the redistribution of $G_\alpha q_{11}$ subunits into the cytosol of HEK293-AT1-WT cells and this redistribution was inhibited by pretreatment with candesartan (Fig. 3a), suggesting that $G_\alpha q_{11}$ is activated by mechanical stretch as well as by AII.

To determine whether an interaction between the AT1 receptor and G proteins has a role in the activation of ERKs, we transfected an AT1 receptor mutant that does not couple to G proteins (AT1-i2m)[22] into COS7 cells. Activation of ERKs by mechanical stretch was weaker in the AT1-i2m-transfected cells than in those overexpressing AT1-WT (Fig. 3b), suggesting that coupling of G proteins to the AT1 receptor is partly involved in the stretch-induced activation of ERKs.

Non-receptor-type tyrosine kinases such as the Janus kinase (Jak) family and the Src family may be important in AT1 receptor signalling[22,23]. The AT1 receptor activates the Src–Ras–ERK pathway independently of G-protein coupling through the association and activation of Jak2 (refs 22,24,25). Mechanical stretch induced association of Jak2 with the AT1 receptor (Fig. 3c) and phosphorylation of Jak2 (Fig. 3d) in HEK293-AT1-WT cells. Pretreatment of the cells with candesartan significantly suppressed association with the AT1 receptor and phosphorylation of Jak2 (Fig. 3c, d). Mechanical stretch did not activate ERKs in HEK293-AT1-WT cells that had been pretreated with AG490, a specific inhibitor of Jak2 (Fig. 3e), or in COS7 cells expressing an AT1-mutant (AT1-mut2)[25] that lacks a binding domain for Jak2 (Fig. 3f). These results suggest that activation of Jak2 is crucially involved in the stretch-induced activation of ERKs.

Mechanical stretch upregulates inositol phosphates

To identify other stretch-induced events, we examined the accumulation of inositol phosphates in COS-7 cells expressing AT1-WT. Overexpression of AT1-WT resulted in a roughly fivefold increase in basal inositol phosphates, as compared with untransfected cells (Fig. 4). Mechanical stretch of these AT1-WT-expressing cells further upregulated inositol phosphate production by about twofold (Fig. 4). Stretching the parental COS7 cells did not increase inositol phosphate production (data not shown). Candesartan inhibited the accumulation of inositol phosphates in COS7 cells expressing AT1-WT, as well as the stretch-induced increase in inositol phosphate production (Fig. 4).

Load-induced cardiac hypertrophy through AT1 receptor

We examined whether mechanical stress could induce cardiac hypertrophy *in vivo* through the AT1 receptor in the absence of AII. We imposed a pressure overload on the heart by constricting the transverse aorta (TAC) of adult male *ATG*$^{-/-}$ mice. Pressure overload for 2 weeks induced significant hypertrophy in the heart of the *ATG*$^{-/-}$ mice (Fig. 5a, b). Heart weight was increased from 110 ± 12 mg to 189 ± 14 mg after 2 weeks of pressure overload (Fig. 5b).

Although treatment with candesartan did not reduce blood pressure in the right carotid artery (sham operated, 78 ± 10 mmHg; TAC plus saline, 166 ± 15 mmHg; TAC plus candesartan, 160 ± 17 mmHg), the development of cardiac hypertrophy was significantly attenuated by candesartan (heart weight, 145 ± 21 mg; Fig. 5). These results suggest that mechanical stress can induce cardiac hypertrophy *in vivo* by activating the AT1 receptor without the involvement of AII.

DISCUSSION

Many basic and clinical studies have shown that RAS is crucially involved in the development of various cardiovascular diseases[9–12]. Much evidence has indicated that RAS exists in various organs, as well as in the circulation, and that local RAS has an important role in organ damage including cardiac hypertrophy[26,27]. All components of RAS, such as angiotensinogen, renin, angiotensin-converting enzyme and receptors, are present in the heart[26,27], and AII induces hypertrophy of cultured cardiomyocytes[27]. It has been reported that AII is stored in cardiomyocytes and that mechanical stretch induces the secretion of stored AII into the culture medium, resulting in the induction of cardiomyocyte hypertrophy by the autocrine mechanism[6]. Taking these observations together, haemodynamic overload has been thought to promote cardiac hypertrophy by inducing the secretion of AII in the heart. In this study, however, we have shown that mechanical stress can induce cardiomyocyte hypertrophy both *in vitro* and *in vivo* through the AT1 receptor without the involvement of AII.

Although mechanical stretch has been reported to induce the release of endogenous AII from cardiomyocytes[6], by radioimmunoassay we did not detect a significant increase in AII in the cul-

a

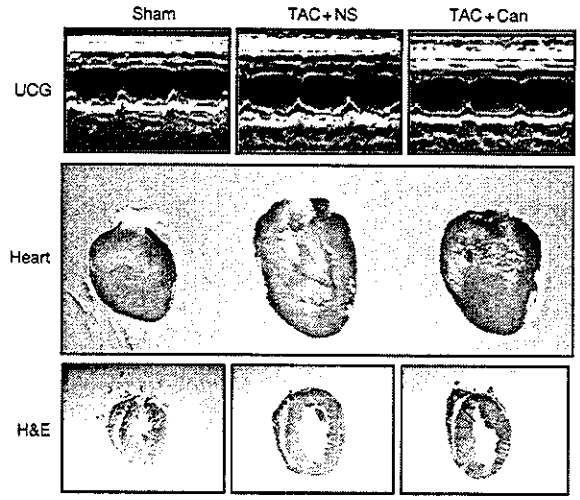

b

	Sham	TAC+NS	TAC+Can
BW (g)	30.8±2.0	32.9±1.2	33.0±1.0
HR (bpm)	477±32	411±65	444±50
IVSTd (mm)	0.75±0.04	1.20±0.06*	0.88±0.04†
LVPWTd (mm)	0.68±0.06	1.12±0.06*	0.86±0.12†
LVIDd (mm)	3.36±0.30	4.07±0.52	3.97±0.30
LVIDs (mm)	1.73±0.21	2.15±0.17	2.10±0.37
EF (%)	85.6±5.0	86.3±3.0	82.7±5.0
HW (mg)	110±12	189±14*	145±21†
BP (mmHg)	78±10	166±15*	160±17*

Figure 5 Cardiac hypertrophy in *ATG*$^{-/-}$ mice induced by pressure overload. Ten-week-old male *ATG*$^{-/-}$ mice, treated with saline (NS) or candesartan (Can), were subjected to a sham or TAC operation. Echocardiography and catheterization were done 2 weeks later. (a) Top, M-mode echocardiograms; middle, gross appearance of the heart; bottom, sections stained by H&E. (b) Echocardiographic results and haemodynamic parameters, shown as the mean ± s.e.m. ($n = 3$). *$P <$ 0.05 versus sham operated; †$P < 0.05$ versus saline. BW, body weight; HR, heart rate; IVSTd, thickness of interventricular septum at diastole; LVPWTd, posterior wall thickness of LV at diastole; LVIDd and LVIDs, LV internal dimension at end diastole and systole, respectively; EF, ejection fraction; HW, heart weight; BP, systolic blood pressure.

ture medium after stretch. AII concentration varied considerably in the conditioned media, whereas the degree of ERK activation induced by stretch was constant, which also suggests that secreted AII is not involved in the stretch-induced activation of ERKs. A very sensitive bioassay, as well as radioimmunoassay, showed that the concentration of AII in medium conditioned by stretch was less than 10^{-11} M, which is far too low to evoke a hypertrophic response in cardiomyocytes. The reason for the difference in the role of secreted AII by stretch between the previous report[6] and this study is not clear at present. Many reports have shown that cardiomyocytes contain about 10^{-13} mol of AII per gram of cells[28–30]. Thus, even if all of the AII stored in cardiomyocytes were secreted by stretch, at most about 10^{-11} M AII would be detected in the culture medium. We detected roughly 2×10^{-12} M AII in culture medium conditioned by stretch for 8 min, consistent with the theoretical concentrations.

Although it is evident that mechanical stress is the primary trigger of cardiac hypertrophy, it is not clear how mechanical stress is received and converted into the active intracellular signalling responsible for the development of cardiac hypertrophy. Muscle LIM protein, integrins and their associated signalling machinery have been reported to be sensors for mechanical stress[31,32]. We propose that the AT1 receptor is also a receptor for mechanical stress. Mechanical stretch did not activate ERKs in HEK293 cells or COS7 cells, but expression of the AT1 receptor gave these cells the ability to respond to stretch. Bioassays using conditioned medium and RT–PCR analysis showed that there is little or no AII in HEK293 cells or COS7 cells. These results suggest that the AT1 receptor is a 'mechanical sensor' and converts mechanical stress into biochemical signals inside the cells.

This hypothesis was confirmed by results from cells expressing the AT1-mut1, which cannot bind AII, and from cardiomyocytes pre-

pared from *ATG*$^{-/-}$ mice. Although AII did not activate ERKs in cells expressing AT1-mut1, mechanical stretch activated ERKs in these cells and this activation was inhibited by an AT1 receptor blocker, candesartan. Mechanical stretch activated ERKs in cardiomyocytes prepared from *ATG*$^{-/-}$ mice, which do not express AII, and candesartan inhibited this activation.

Because mechanical stretch did not activate ERKs in cells expressing the ET1A or β2-AR receptors, not all GPCRs are necessarily a mechanical sensor. Although we do not know at present why the AT1 receptor, but not the ET1A or β2-AR receptor, is significantly activated by mechanical stretch, there are a few possibilities. First, specificity may be due to molecules that associate with the AT1 receptor. We found that in the response to mechanical stretch, some unknown molecules bind to the AT1 receptor (our own unpublished results). Second, diversity in the structures and expression of the receptors may also determine their responsibility to mechanical stress[16,27,33].

After binding to AII, the AT1 receptor changes its conformation into an active form and stimulates G proteins through its intracellular domains[15,20,33,34]. The intracellular loops and the region between residues 312 and 318 in the carboxy-terminal tail of the AT1 receptor have been reported to be essential for coupling and activating G proteins[35]. After activation, G proteins dissociate into α- and βγ-subunits, and the α-subunit is translocated into the cytosol[34]. In addition, ligand binding to the AT1 receptor induces association of the C terminus of the AT1 receptor with Jak2, thereby resulting in activation of the Jak2–STAT3 pathway[22–25]. Although there is no direct evidence, our results suggest that, similar to AII binding to the AT1 receptor, mechanical stress induces a conformational change in the AT1 receptor by a mechanism independent of AII binding, resulting in the association and activation of G proteins and Jak2.

There are a few mechanisms by which mechanical stress might activate the AT1 receptor without the involvement of AII. First, stretching the cell membrane may directly change the conformation of the AT1 receptor. Many receptors can change their conformation between the active and inactive state under basal conditions without ligands[36,37]. Candesartan reduced the basal activity of ERKs, suggesting that part of the wild-type AT1 receptor is in an active state, and mechanical stress may increase the number of AT1 receptors in the active state. Second, mechanical stretch might activate specific mechanical sensors, which then activate the AT1 receptor from inside the cells. Potential stretch sensors, such as muscle LIM protein, integrins and stretch-sensitive ion channels, might activate the AT1 receptor, though the underlying mechanism remains to be determined.

Strong pressure overload induced cardiac hypertrophy in *ATG*$^{-/-}$ mice, indicating that mechanical stress can induce cardiac hypertrophy without AII. Treatment with candesartan significantly attenuated the development of cardiac hypertrophy without reducing blood pressure, suggesting that mechanical stress activates the AT1 receptor and induces cardiac hypertrophy without the involvement of AII *in vivo*. We previously reported that pressure overload induces cardiac hypertrophy in AT1a receptor knockout mice[38]. The activity of tyrosine kinases is upregulated before stretch and more strongly enhanced by mechanical stretch in AT1a-receptor-deficient cardiomyocytes as compared with wild-type cells through epidermal growth factor (EGF) receptor tyrosine kinases[39], suggesting that the AT1 receptor is not indispensable for stretch-induced cardiac hypertrophy and that some compensatory mechanisms operate and induce cardiac hypertrophy even in the absence of the AT1 receptor[38,39].

Candesartan reduced the basal activity of ERKs and inositol phosphates in cells overexpressing AT1-WT and inhibited the stretch-induced activation of ERKs and increase in inositol phosphates independently of AII, suggesting that candesartan works as an inverse agonist of the AT1 receptor. An inverse agonist of the AT1 receptor is defined as an agent that stabilizes the AT1 receptor in an inactive conformation, thereby inhibiting signals evoked by the wild-type or active AT1 receptor. As an inverse agonist, candesartan may inhibit changes in conformation of AT1 receptor and thus may efficiently suppress its activation induced by both mechanical stress and AII. Much evidence suggests that local RAS has a crucial role in injury to various organs[26,27,40]. It remains to be determined whether activation of the AT1 receptor without AII occurs in other organs, and whether inverse agonists prevent organ damage more effectively than do competitive antagonists. □

METHODS

cDNA constructs. The AT1a receptor mutants lacking binding activity with AII (AT1-mut1) or the Jak2 coupling domain (AT1-mut2) were generated by PCR from the wild-type mouse AT1 receptor (GenBank accession number S37484)[41] by replacement of Lys 199 with glutamine[13] or truncation of the C terminus (residues 312–359)[22], respectively. AT1-i2m[22], β2-AR[42] and ET1A[43] were gifts from J. Sadoshima, R J. Lefkowitz and S. Kimura, respectively. The complementary DNAs used in this study are summarized in Supplementary Information, Table 1.

Cell culture and transfection. We prepared primary cultures of cardiomyocytes from the ventricles of 1-day-old Wistar rats or *ATG*$^{-/-}$ mice as described[19]. Adult and neonatal cardiomyocytes of *ATG*$^{-/-}$ mice were prepared as described[44]. HEK293 and COS7 cells were cultured in Dulbecco's modified Eagle's medium with 10% serum. cDNAs were transfected by the calcium phosphate method as described[19]. Stable transformants were selected by the addition of hygromycin B to the cells 3 d after transfection and for all subsequent passages of the cells[41]. All cultures were transferred to serum-free conditions 48 h before stimulation.

Western blotting. Total proteins (50 μg) were size-fractionated by SDS–PAGE and transferred to Immobilon-P membranes (Millipore). The blotted membranes were incubated with antibodies against phosphorylated ERKs, phosphorylated Jak2, Jak2, AT1 or $G_{\alpha q/11}$ (Santa Cruz).

***ATG* gene expression.** Expression of the *ATG* gene was examined by RT–PCR using specific primers (sense, 5'-TTCAGGCCAAGACCTCCC-3'; antisense, 5'-CCAGCCGGGAGGTGCAGT-3')[45]. We separated the PCR products on 1.2% agarose gels and visualized them by using ethidium bromide.

Detection of inositol phosphates. Accumulation of inositol phosphates was assayed in COS7 cells as described[46,47]. In brief, 24 h after transfection by the DEAE–adenovirus method[48], cells were replated in 24-well plates at 1.5×10^5 cells per well and labelled for 24 h with myo-[^{3}H]inositol (2 μCi ml^{-1}; Amersham). The cells were washed in medium containing 5 mM LiCl for 10 min, incubated with vehicle or candesartan for 5 h, and then subjected to mechanical stretch for 45 min in the presence of 5 mM LiCl. Inositol phosphates and total inositol fractions were resolved on a Dowex AG 1-X8 formate column (Bio-Rad), and inositol phosphate accumulation was estimated by determining the ratio of inositol phosphate radioactivity to the sum of inositol phosphate plus inositol radioactivity.

AII in the medium of cultured cardiomyocytes. Culture medium (2 ml per dish) was collected from dishes before and after stretching the cells by 20% for 8 min. We measured AII concentration by radioimmunoassay using two antibodies specific for AII (SRL Co.).

TAC operation. TAC operation was done on 10-week-old male *ATG*$^{-/-}$ mice and wild-type C52/BL6 mice[14]. A mini-osmotic pump (Alzet) filled with saline or candesartan was implanted subcutaneously in mice 3 d before TAC. All mouse protocols were approved by the guidelines of Chiba University.

Haemodynamic parameters. Transthoratic echocardiography (UCG) was done as reported[38] using a Agilent sonos 4500 (Agilent Technologies Co.) equipped

with a 11-MHz imaging transducer. Haemodynamic measurements were taken by inserting a micronanometer catheter (Millar 1.4F, SPR 671, Millar Instruments) from the right common carotid artery into the aorta and then the left ventricle (LV). The transducer was connected to the MacLab system (AD Instruments) to record the pressure. For heart morphometry, hearts were perfused with 10% buffered formalin and subsequently embedded in paraffin, sectioned and stained with haematoxylin and eosin (H&E).

Statistics. Data are shown as mean ± s.e.m. Multiple group comparison was done by a one-way analysis of variance (ANOVA), followed by the Bonferroni procedure for comparison of means. A two-tailed Student's *t*-test was used to compare drug-treated and vehicle-treated specimens under identical conditions. Values of $P < 0.05$ were considered statistically significant.

Note: Supplementary Information is available on the Nature Cell Biology website.

ACKNOWLEDGEMENTS

We thank R. J. Lefkowitz, J. Sadoshima and S. Kimura for plasmids; S.-i. Miura for advice; and A. Okubo, E. Fujita, R. Kobayashi and M. Watanabe for technical support. This work was supported by a Grant-in-Aid for Scientific Research, Developmental Scientific Research, and Scientific Research on Priority Areas from the Ministry of Education, Science, Sports, and Culture; and by a grant for research on life science from Uehara Memorial Foundation, Japan (to I.K.).

COMPETING FINANCIAL INTERESTS

The authors declare that they have no competing financial interests.

Received 25 March 2004; accepted 19 April 2004
Published online at http://www.nature.com/naturecellbiology.

1. Levy, D., Garrison, R. J., Savage, D. D., Kannel, W. B. & Castelli, W. P. Prognostic implications of echocardiographically determined left ventricular mass in the Framingham heart study. *N. Eng. J. Med.* **322**, 1561–1566 (1990).
2. Chien, K. R., Grace, A. A. & Hunter, J. J. Molecular biology of cardiac hypertrophy and heart failure. In *Molecular Basis of Cardiovascular Disease* (ed. K. R. Chien) 211–250 (W. B. Saunders, Philadelphia, PA, 1998).
3. Komuro, I. *et al.* Stretching cardiac myocytes stimulates protooncogene expression. *J. Biol. Chem.* **265**, 3595–3598 (1990).
4. Sadoshima, J., Jahn, L., Takahashi, T., Kulik, T. J. & Izumo, S. Molecular characterization of the stretch-induced adaptation of cultured cardiac cells. An *in vitro* model of load-induced cardiac hypertrophy. *J. Biol. Chem.* **267**, 10551–10560 (1992).
5. Komuro, I. & Yazaki, Y. Control of cardiac gene expression by mechanical stress. *Annu. Rev. Physiol.* **55**, 55–75 (1993).
6. Sadoshima, J., Xu, Y., Slayter, H. S. & Izumo, S. Autocrine release of angiotensin II mediates stretch-induced hypertrophy of cardiac myocytes *in vitro*. *Cell* **75**, 977–984 (1993).
7. Yamazaki, T. *et al.* Angiotensin II partly mediates mechanical stress-induced cardiac hypertrophy. *Circ. Res.* **77**, 258–265 (1995).
8. Kojima, M. *et al.* Angiotensin II receptor antagonist TCV-116 induces regression of hypertensive left ventricular hypertrophy *in vivo* and inhibits the intracellular signaling pathway of stretch-mediated cardiomyocyte hypertrophy *in vitro*. *Circulation* **89**, 2204–2211 (1994).
9. Griendling, K. K., Lassegue, B. & Alexander, R. W. Angiotensin receptors and their therapeutic implications. *Annu. Rev. Pharmacol. Toxicol.* **36**, 281–306 (1996).
10. Pitt, B. *et al.* Effect of losartan compared with captopril on mortality in patients with symptomatic heart failure: randomised trial—the Losartan Heart Failure Survival Study ELITE II. *Lancet* **355**, 1582–1587 (2000).
11. Cohn, J. N. *et al.* A randomized trial of the angiotensin-receptor blocker valsartan in chronic heart failure. *N. Eng. J. Med.* **345**, 1667–1675 (2001).
12. Lindholm, L. H. *et al.* Cardiovascular morbidity and mortality in patients with diabetes in the Losartan Intervention For Endpoint reduction in hypertension study (LIFE): a randomised trial against atenolol. *Lancet* **359**, 1004–1010 (2002).
13. Yamano, Y., Ohyama, K., Chaki, S., Guo, D. F. & Inagami, T. Identification of amino acid residues of rat angiotensin II receptor for ligand binding by site directed mutagenesis. *Biochem. Biophys. Res. Comm.* **187**, 1426–1431 (1992).
14. Tanimoto, K. *et al.* Angiotensinogen-deficient mice with hypotension. *J. Biol. Chem.* **269**, 31334–31337 (1994).
15. van Biesen, T., Luttrell, L. M., Hawes, B. E. & Lefkowitz, R. J. Mitogenic signaling via G protein-coupled receptors. *Endocr. Rev.* **17**, 698–714 (1996).
16. Rockman, H. A., Koch, W. J. & Lefkowitz, R. J. Seven-transmembrane-spanning receptors and heart function. *Nature* **415**, 206–212 (2002).
17. Bockaert, J. & Pin, J. P. Molecular tinkering of G protein-coupled receptors: an evolutionary success. *EMBO J.* **18**, 1723–1729 (1999).
18. Yamazaki, T. *et al.* Endothelin-1 is involved in mechanical stress-induced cardiomyocyte hypertrophy. *J. Biol. Chem.* **271**, 3221–3228 (1996).
19. Zou, Y. *et al.* Both G_s and G_i proteins are critically involved in isoproterenol-induced cardiomyocyte hypertrophy. *J. Biol. Chem.* **274**, 9760–9770 (1999).
20. Bernstein, K. E. & Alexander, R. W. Counterpoint: molecular analysis of the angiotensin II receptor. *Endocr. Rev.* **13**, 381–386 (1992).
21. Inagami, T. Molecular biology and signaling of angiotensin receptors: an overview. *J. Am. Soc. Nephrol.* **11**, S2–S7 (1999).
22. Seta, K., Nanamori, M., Modrall, J. G., Neubig, R. R. & Sadoshima, J. AT1 receptor mutant lacking heterotrimeric G protein coupling activates the Src–Ras–ERK pathway without nuclear translocation of ERKs. *J. Biol. Chem.* **277**, 9268–9277 (2002).
23. Marrero, M. B. *et al.* Direct stimulation of Jak/STAT pathway by the angiotensin II AT1 receptor. *Nature* **375**, 247–250 (1995).
24. Ali, M. S. *et al.* Dependence on the motif YIPP for the physical association of Jak2 kinase with the intracellular carboxyl tail of the angiotensin II AT1 receptor. *J. Biol. Chem.* **272**, 23382–23388 (1997).
25. Ali, M. S., Sayeski, P. P. & Bernstein, K. E. Jak2 acts as both a STAT1 kinase and as a molecular bridge linking STAT1 to the angiotensin II AT1 receptor. *J. Biol. Chem.* **275**, 15586–15593 (2000).
26. Lee, M. A., Bohm, M., Paul, M. & Ganten, D. Tissue renin–angiotensin systems. Their role in cardiovascular disease. *Circulation* **87**, 7–13 (1993).
27. Baker, K. M., Booz, G. W. & Dostal, D. E. Cardiac actions of angiotensin II: role of an intracardiac renin–angiotensin system. *Annu. Rev. Physiol.* **54**, 227–241 (1992).
28. Mazzolai, L. *et al.* Increased cardiac angiotensin II levels induce right and left ventricular hypertrophy in normotensive mice. *Hypertension* **35**, 985–991 (2000).
29. Wei, C. C. *et al.* Differential ANG II generation in plasma and tissue of mice with decreased expression of the ACE gene. *Am. J. Physiol.* **282**, H2254–H2258 (2002).
30. Campbell, D. J. *et al.* Effect of reduced angiotensin-converting enzyme gene expression and angiotensin-converting enzyme inhibition on angiotensin and bradykinin peptide levels in mice. *Hypertension* **43**, 1–6 (2004).
31. Knoll, R. *et al.* The cardiac mechanical stretch sensor machinery involves a Z disc complex that is defective in a subset of human dilated cardiomyopathy. *Cell* **111**, 943–955 (2002).
32. Brancaccio, M. *et al.* Melusin, a muscle-specific integrin β1-interacting protein, is required to prevent cardiac failure in response to chronic pressure overload. *Nature Med.* **9**, 68–75 (2003).
33. Karnik, S. S., Gogonea, C., Patil, S., Saad, Y. & Takezako, T. Activation of G-protein-coupled receptors: a common molecular mechanism. *Trends Endocrinol. Metab.* **14**, 431–437 (2004).
34. Akhter, S. A. *et al.* Targeting the receptor-G_q interface to inhibit *in vivo* pressure overload myocardial hypertrophy. *Science* **280**, 574–577 (1998).
35. Sano, T. *et al.* A domain for G protein coupling in carboxyl-terminal tail of rat angiotensin II receptor type 1A. *J. Biol. Chem.* **272**, 23631–23636 (1997).
36. Lefkowitz, R. J., Cotecchia, S., Samama, P. & Costa, T. Constitutive activity of receptors coupled to guanine nucleotide regulatory proteins. *Trends Pharmacol. Sci.* **14**, 303–307 (1993).
37. Leurs, R., Smit, M. J., Alewijnse, A. E. & Timmerman, H. Agonist-independent regulation of constitutively active G-protein-coupled receptors. *Trends Biochem. Sci.* **23**, 418–422 (1998).
38. Harada, K. *et al.* Acute pressure overload could induce hypertrophic responses in the heart of angiotensin II type 1a knockout mice. *Circ. Res.* **82**, 779–785 (1998).
39. Kudoh, S. *et al.* Mechanical stretch induces hypertrophic responses in cardiac myocytes of angiotensin II type 1a receptor knockout mice. *J. Biol. Chem.* **273**, 24037–24043 (1998).
40. Bader, M. *et al.* Tissue renin–angiotensin systems: new insights from experimental animal models in hypertension research. *J. Mol. Med.* **79**, 76–102 (2001).
41. Ishida, J. *et al.* Expression and characterization of mouse angiotensin II type 1a receptor tagging hemagglutinin epitope in cultured cells. *Int. J. Mol. Med.* **3**, 263–270 (1999).
42. Daaka, Y., Luttrell, L. M. & Lefkowitz, R. J. Switching of the coupling of the β2-adrenergic receptor to different G proteins by protein kinase A. *Nature* **390**, 88–91 (1997).
43. Sakurai, T. *et al.* Cloning of a cDNA encoding a non-isopeptide-selective subtype of the endothelin receptor. *Nature* **348**, 732–735 (1990).
44. Sambrano, G. R. *et al.* Navigating the signalling network in mouse cardiac myocytes. *Nature* **420**, 712–714 (2002).
45. Malhotra, R., Sadoshima, J., Brosius, F. C. & Izumo, S. Mechanical stretch and angiotensin II differentially upregulated the renin–angiotensin system in cardiac myocytes *in vitro*. *Circ. Res.* **85**, 137–146 (1999).
46. Conklin, B. R., Chabre, O., Wong, Y. H., Federman, A. D. & Bourne, H. R. Recombinant $G_q\alpha$. Mutational activation and coupling to receptors and phospholipase C. *J. Biol. Chem.* **267**, 31–34 (1992).
47. Iiri, T., Bell, S. M., Baranski, T. J., Fujita, T. & Bourne, H. R. A $G_s\alpha$ mutant designed to inhibit receptor signaling through Gs. *Proc. Natl. Acad. Sci. USA* **96**, 499–504 (1999).
48. Garcia, P. D., Onrust, R., Bell, S. M., Sakmar, T. P. & Bourne, H. R. Transducin-α C-terminal mutations prevent activation by rhodopsin: a new assay using recombinant proteins expressed in cultured cells. *EMBO J.* **14**, 4460–4469 (1995).

Case Report

Steroid-responsive thromboangiitis obliterans

Atsuhiko T Naito, Tohru Minamino, Kaoru Tateno, Toshio Nagai, Issei Komuro

Lancet 2004; 364: 1098

Department of Cardiovascular Science and Medicine (A T Naito MD, T Minamino MD, K Tateno MD, T Nagai MD, I Komuro MD) Chiba University Graduate School of Medicine, 1-8-1 Inohana, Chuo-ku, Chiba 260-8670, Japan

Correspondence to: Dr Issei Komuro komuro-tky@umin.ac.jp

A 41-year-old, non-smoking man came to the emergency room in June, 2003, complaining of cold, painful hands. On examination, we found nothing abnormal, apart from cyanotic, tender fingers, with poor perfusion as shown on by laser doppler and infrared thermography (figure). Blood tests showed eosinophilia; 3097/μL, and eosinophilic cationic protein (ECP), >150 μg/mL (normal <14·7 μg/mL). Acute-phase reactants, C-reactive protein and the erythrocyte sedimentation rate were within normal limits. Chest radiographs and echocardiography showed no abnormalities or evidence of eosinophilia-induced end-organ damage. Angiography showed occlusion of the distal arteries of upper and lower extremities. We searched for parasitic infections and malignancy, to no avail. We excluded vasculitis from our differential diagnosis when the results of immunological tests showed no antinuclear, anticentromere, anticardiolipin, anti-dsDNA, anti-Scl70, anti-SS-A, anti-RNP, and anti-Jo1 antibodies, rheumatoid factor, ANCA, or cryoglobulins. Serum tryptase level was low; 3·9 ng/mL, indicating no involvement of mast cells. Our patient thus fulfilled the Japanese criteria for thromboangiitis obliterans,[1,2] and we started treatment with intravenous heparin and alprostadil. The patient's digital ischaemia and intermittent claudication showed no improvement after 1 week and his middle finger became necrotic. At that point, his eosinophil count was 5014/μL. We decided to give him prednisolone 30 mg daily, to treat the eosinophilia, in case it was contributing to the distal arterial occlusion. After 2 weeks of treatment, his eosinophil count and serum ECP levels decreased to 185/mm^3 and 19·5 μg/mL, respectively. Laser doppler and infrared thermography showed a clear improvement in digital ischaemia (figure). When last seen in April, 2004, his fingers were completely healed, and he had no complaints of claudication.

A 62-year-old non-smoking man had been diagnosed with thromboangiitis obliterans in October, 1997, on the basis of angiography that showed occlusion of distal arteries in the absence of atherosclerosis. For 6 years, he had been treated with beraprost, anti-coagulants, lumbar sympathetic block, and continuous epidural block, but digital necrosis and pain persisted. He was admitted to our hospital in September, 2003. Blood tests showed eosinophilia; 2300/μL and ECP; 107 μg/mL. Tests for other causes of vascuolopathy were negative. We treated him with prednisolone, 30 mg daily, and after 2 weeks, his eosinophil count was 185/mm^3 and serum ECP was 25·8 μg/mL. His pain had disappeared and his digital ischaemia largely resolved by the time of discharge in December, 2003.

Both of these patients fulfilled the Japanese criteria for thromboangiitis obliterans, but they were atypical patients because they were non-smokers at the onset of the symptoms. Current history of smoking is included in many case definitions of thromboangiitis obliterans.[1] Stopping smoking is the only proven strategy to prevent the progression of this disease, but 6·8% of Japanese patients diagnosed with thromboangiitis obliterans are non-smokers.[2] Hypereosinophilia causes end-organ damage by inducing thrombosis and endothelial damage, and simultaneous presentations of thromboangiitis obliterans with eosinophilia due to temporal arteritis have been reported.[3-5] However, we could find no reports of distal artery occlusion consistent with thromboangiitis obliterans and eosinophilia that responded to steroids. It will be interesting to see if patients who are diagnosed with thromboangiitis obliterans include a subset that have steroid-responsive disease, mediated by eosinophilia.

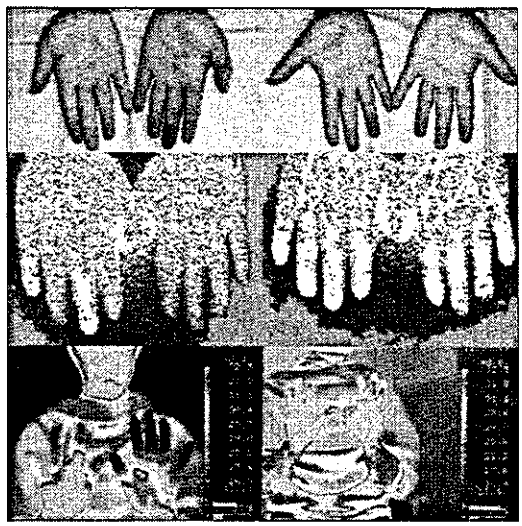

Figure: Photograph (top), laser doppler (middle), and infrared thermography (bottom), showing digital ischaemia before (left) and after steroid therapy (right).

References

1 Olin JW. Thromboangiitis obliterans (Buerger's disease). *N Engl J Med* 2000; 343: 864–69.

2 Sasaki S, Sakuma M, Yasuda K. Current status of thromboangiitis obliterans (Buerger's disease) in Japan. *Int J Cardiol* 2000; 75: S175–81.

3 Lie JT, Michet CJ Jr. Thromboangiitis obliterans with eosinophilia (Buerger's disease) of temporal arteries. *Hum Pathol* 1988; 19: 598–602.

4 Fujimoto M, Sato S, Hayashi N, Wakugawa M, Tsuchida T, Tamaki K. Juvenile temporal arteritis with eosinophilia: a distinct clinicopathological entity. *Dermatology* 1996; 192: 32–35.

5 Ferguson GT, Starkebaum G. Thromboangiitis obliterans associated with idiopathic hypereosinophilia. *Arch Intern Med* 1985; 145: 1726–28.

Vasorin, a transforming growth factor β-binding protein expressed in vascular smooth muscle cells, modulates the arterial response to injury *in vivo*

Yuichi Ikeda*†‡, Yasushi Imai†, Hidetoshi Kumagai*§, Tetsuya Nosaka*, Yoshihiro Morikawa¶, Tomoko Hisaoka¶, Ichiro Manabe†, Koji Maemura†, Takashi Nakaoka‖, Takeshi Imamura**, Kohei Miyazono††, Issei Komuro‡‡, Ryozo Nagai†, and Toshio Kitamura*‡§§

Divisions of *Hematopoietic Factors and §§Cellular Therapy and ‖Department of Advanced Medicine, Institute of Medical Science, University of Tokyo, Tokyo 108-8639, Japan; Departments of †Cardiovascular Medicine and ††Molecular Pathology, Graduate School of Medicine, University of Tokyo, Tokyo 113-8655, Japan; §Takada Research Laboratories, Chugai Pharmaceutical Company, Limited, Tokyo 171-8545, Japan; ¶Department of Anatomy and Neurobiology, Wakayama Medical School, Wakayama 641-8509, Japan; **Department of Biochemistry, Cancer Institute of the Japanese Foundation for Cancer Research, Tokyo 170-8455, Japan; and ‡‡Department of Cardiovascular Science and Medicine, Graduate School of Medicine, Chiba University, Chiba 260-8670, Japan

Communicated by Masashi Yanagisawa, University of Texas Southwestern Medical Center, Dallas, TX, June 9, 2004 (received for review February 25, 2004)

Growth factors, cell-surface receptors, adhesion molecules, and extracellular matrix proteins play critical roles in vascular pathophysiology by affecting growth, migration, differentiation, and survival of vascular cells. In a search for secreted and cell-surface molecules expressed in the cardiovascular system, by using a retrovirus-mediated signal sequence trap method, we isolated a cell-surface protein named vasorin. Vasorin is a typical type I membrane protein, containing tandem arrays of a characteristic leucine-rich repeat motif, an epidermal growth factor-like motif, and a fibronectin type III-like motif at the extracellular domain. Expression analyses demonstrated that vasorin is predominantly expressed in vascular smooth muscle cells, and that its expression is developmentally regulated. To clarify biological functions of vasorin, we searched for its binding partners and found that vasorin directly binds to transforming growth factor (TGF)-β and attenuates TGF-β signaling *in vitro*. Vasorin expression was down-regulated during vessel repair after arterial injury, and reversal of vasorin down-regulation, by using adenovirus-mediated *in vivo* gene transfer, significantly diminished injury-induced vascular lesion formation, at least in part, by inhibiting TGF-β signaling *in vivo*. These results suggest that down-regulation of vasorin expression contributes to neointimal formation after vascular injury and that vasorin modulates cellular responses to pathological stimuli in the vessel wall. Thus, vasorin is a potential therapeutic target for vascular fibroproliferative disorders.

Vascular smooth muscle cells (VSMCs), the major cell type in the vessel wall, show a spectrum of phenotypes, depending on environmental cues. Various injurious stimuli provoke the proliferation of differentiated medial VSMCs, which migrate to the intima and produce extracellular matrix proteins, resulting in the narrowing of the vascular lumen. These processes, called VSMC phenotypic modulation, play a key role in development of atherosclerotic diseases, such as postangioplasty restenosis, vein graft disease, and transplant vasculopathy. Whereas tremendous progress has been made in identifying growth factors and transcription factors that regulate the vascular response to injury, much information is lacking regarding cell-surface molecules that are involved in the pathogenesis of vascular fibroproliferative disorders. The signal sequence trap (SST) is a strategy to identify cDNAs containing signal sequence that encode secreted and type I membrane proteins (1, 2). We recently developed a refined SST system based on retrovirus-mediated expression screening (SST-REX) (3). In a search for secreted and cell-surface molecules expressed in the cardiovascular system, by using SST-REX, we identified a TGF-β binding protein, vasorin. Vasorin is predominantly expressed in VSMCs and modulates the vascular response to injury, at least in part, by attenuating TGF-β signaling *in vivo*. Here, we describe the molecular and functional characteristics of vasorin.

Methods

Cells and Reagents. A murine pro-B cell line Ba/F3 was maintained in RPMI medium 1640 containing 10% FCS and 2 ng/ml murine IL-3 (R & D Systems). Chinese hamster ovary (CHO) cells were grown in DMEM supplemented with 5% FCS and 1% nonessential amino acids (Invitrogen). Stable transfectants were established by the retrovirus expression system, by using a bicistronic retroviral vector pMX-IRES-EGFP as reported (4). Rat aortic VSMCs, prepared from 8-week-old Wistar rats by using the explant method (5), were grown in DMEM supplemented with 10% FCS. Primary antibodies used in this study were anti-Flag monoclonal antibody (M2, Sigma), anti-Smad2/3 monoclonal antibody (BD Transduction Laboratories), anti-phospho-Smad2 polyclonal antibody (Upstate, Charlottesville, VA), and anti-rat CD45 monoclonal antibody (BD Pharmingen).

Screening of a Human Heart cDNA Library by SST-REX and Cloning of the Full-Length cDNA Encoding *Vasorin*. A human heart cDNA library was screened by SST-REX as described (3). Briefly, cDNA was synthesized from poly(A)$^+$ RNA of human hearts (Clontech), by using the SuperScript Choice system (Invitrogen). The synthesized cDNA was separated based on size, and fractions >600 bp were inserted into *Bst*XI sites of the pMX-SST vector, by using *Bst*XI adapters (Invitrogen). Ba/F3 cells were infected with high-titer retroviruses expressing the human heart cDNA library, and the integrated cDNA fragments were isolated from factor-independent Ba/F3 clones by genomic PCR. All cDNA fragments were sequenced and analyzed. Subsequently, a human heart cDNA library in the pME18S vector was screened by using the ^{32}P-labeled cDNA fragment of a clone so as to isolate the entire coding region.

RNA, Protein, and Histological Analyses. Northern blot, *in situ* hybridization, semiquantitative RT-PCR, immunoprecipitation, Western blot, and histological analyses were done as described

Abbreviations: VSMC, vascular smooth muscle cell; TGF, transforming growth factor; EGF, epidermal growth factor; SST, signal sequence trap; SST-REX, retrovirus-mediated SST; CHO, Chinese hamster ovary; RA, retinoic acid; E*n*, embryonic day *n*; LRR, leucine-rich repeat; Ad, adenovirus; Ad-vasorin, Ads expressing vasorin-Flag; PDGF, platelet-derived growth factor.

Data deposition: The sequence reported in this paper has been deposited in the GenBank database (accession no. AY166584).

*To whom correspondence may be addressed at: 4-6-1, Shirokanedai, Minato-ku, Tokyo 108-8639, Japan. E-mail: yikeda-tky@umin.ac.jp or kitamura@ims.u-tokyo.ac.jp.

www.pnas.org/cgi/doi/10.1073/pnas.0404117101